DISCRETE AND CONTINUOUS
DYNAMICAL SYSTEMS SERIES B
Volume **18**, Number **5**, July **2013**

doi:10.3934/dcdsb.2013.18.xx

pp. **X–XX**

A RELAXATION METHOD FOR ONE DIMENSIONAL TRAVELING WAVES OF SINGULAR AND NONLOCAL EQUATIONS

Weiran Sun

Department of Mathematics
Simon Fraser University
8888 University Drive, Burnaby, BC V5A 4Z2, Canada

Min Tang

Department of mathematics and Institute of Natural Sciences
MOE-LSC, Shanghai Jiao Tong University
Shanghai, 200240, China

(Communicated by Benoit Perthame)

Abstract. Recent models motivated by biological phenomena lead to non-local PDEs or systems with singularities. It has been recently understood that these systems may have traveling wave solutions that are not physically relevant [19]. We present an original method that relies on the physical evolution to capture the "stable" traveling waves. This method allows us to obtain the traveling wave profiles and their traveling speed simultaneously. It is easy to implement, and it applies to classical differential equations as well as nonlocal equations and systems with singularities. We also show the convergence of the scheme analytically for bistable reaction diffusion equations over the whole space $\mathbb{R}$.

1. **Introduction.** There is a vast number of biological phenomena where the key elements or precursors to a development process exhibit traveling waves. Classical models describing these phenomena include various reaction-diffusion equations such as the Fisher/KPP and Allen-Cahn equations [13, 15, 23]. More recent models motivated by biological phenomena lead to non-local PDEs or systems with singularities. These models may exhibit traveling waves but the long time behavior of these evolution equations may not always converge to these traveling waves as one might expect. It has been recently understood that there exist unstable traveling waves which are not physically relevant [19]. We present in this paper an original method that relies on the physical evolution to capture the "stable" traveling waves. Our method also gives certain indications about what happens when there does not exist any physically relevant traveling wave.

Recall that traveling wave solutions are special solutions of evolution equations. Specifically, let $u(x,t)$ be a solution to an evolution equation that involves space

2010 *Mathematics Subject Classification.* Primary: 35C07, 35Q92; Secondary: 35K57.
Key words and phrases. Reaction-diffusion equations, traveling wave, numerical simulation.
The second author is supported by NSF of Shanghai 12ZR1445400.

$x \in \mathbb{R}$ and time $t \in \mathbb{R}^+$. If u has a special form such that there exist a function ϕ and a constant σ^* and

$$u(x,t) = \phi(x - \sigma^* t)\,, \tag{1.1}$$

then $u(x,t)$ is called a traveling wave solution. The function ϕ is called the traveling front and σ is the associated traveling speed.

There are several classical ways to simulate traveling wave solutions. The first approach is to work with the evolution equation for $u(x,t)$ and let $u(x,t)$ propagate with time [18, 21, 22]. The second approach is to apply the Newton iteration method to solve the steady state equation for the traveling front ϕ directly after imposing an additional condition $\phi(0) = \epsilon$ [24, 26]. The third way is to reformulate traveling wave equations as first-order ODE systems and apply the method of projection boundary conditions [10, 11]. In general, the first type of methods requires large computational domains and a long time to achieve convergence to the traveling front. Besides, it requires large memory to verify that the front velocity is a constant in time, even if the shape of the front keeps the same. The second and third types of methods rely on the traveling front equation, whose solution might be physically irrelevant in the sense that it might not correctly describe the long time behavior of the original evolution equation. Both methods use the idea of iteration but in a different manner. In general, convergence is not guaranteed for these two methods. When divergence occurs, it is unclear whether this is because traveling wave solutions do not exist, or one needs to improve the algorithm. Furthermore, the third type of methods using ODE systems, to the best of our knowledge, has difficulties to generalize to nonlocal equations.

In this paper, we construct a new numerical method for traveling wave simulations that can avoid the aforementioned difficulties. For simplicity, we illustrate the idea using the scalar reaction-diffusion equation

$$\partial_t u = \partial_{xx} u + f[u]\,, \qquad u : \mathbb{R} \times \mathbb{R}^+ \to \mathbb{R}\,, \tag{1.2}$$

where f is a functional of u that satisfies $f[0] = f[1] = 0$. This type of equations are widely used in the modeling of biological phenomena where different choices of $f[u]$ give different biological models. For example, if $f[u] = u(1-u)$ then equation 1.2 is the most studied Fisher/KPP equation. It was originally derived for the simulation of propagation of a gene in a population [13]. If $f[u] = u(1-u)(u-\alpha)$ where α is a constant between 0 and 1, then equation 1.2 is called the Allen-Cahn model, which takes into account of the strong Allee effect that a population exhibits a critical size and will die out if the initial density is below this critical size. The case when $f[u] = u(1 - \psi * u)$ is the nonlocal Fisher/KPP equation for modeling the population selection. Here $\psi * u$ is the convolution of u with a given kernel ψ. These models are known to possess traveling wave solutions under various conditions (cf. [4, 14, 15, 23]).

In order to study the existence and properties of a traveling wave, we need to find the equation for the traveling front v in 1.1. This equation can be obtained by substituting $v(x') = v(x - \sigma t)$ into 1.2. For the ease of notation, we drop the prime on x' and still use x as the spatial variable. Then $v(x)$ satisfies

$$\sigma^* \partial_x \phi + \partial_{xx} \phi + f[\phi] = 0\,, \qquad \phi : \mathbb{R} \to \mathbb{R}\,. \tag{1.3}$$

For a fixed σ, this is a second order ordinary differential equation in v where the source term f generally is nonlinear or nonlocal. This equation needs to be accompanied with appropriate boundary conditions. Heuristically, the traveling front

connects two steady states and behaves like a transition profile. Under the assumption that $f[0] = f[1] = 0$, equation 1.3 has two steady states $u = 0$ and $u = 1$. In some cases this suggests to impose the boundary conditions

$$\phi(-\infty) = 1\,, \qquad \phi(+\infty) = 0\,. \tag{1.4}$$

There are also other possible boundary conditions. For instance for those systems considered in [22] where one only knows the existence of a steady state but not its explicit form, the following boundary conditions are used:

$$\partial_x\phi(-\infty) = 0\,, \qquad \phi(+\infty) = 0\,. \tag{1.5}$$

Notice that 1.3 with either 1.4 or 1.5 is translation invariant, that is, if $\phi(x)$ is a solution, then $\phi(x-b)$ is also a solution for any $b \in \mathbb{R}$. In order to remove this invariance, as in [24, 26], we introduce another condition $\phi(0) = \epsilon$ to 1.3. Here $0 < \epsilon < 1$ is an arbitrary fixed number. With the boundary conditions in 1.4, the full system now becomes

$$\begin{aligned} &\sigma^*\partial_x\phi + \partial_{xx}\phi + f[\phi] = 0\,, \qquad \phi : \mathbb{R} \to \mathbb{R}\,, \\ &\phi(-\infty) = 1\,, \qquad \phi(+\infty) = 0\,, \qquad \phi(0) = \epsilon\,. \end{aligned} \tag{1.6}$$

The starting point of our method is based on 1.6 instead of the evolution equation 1.2. The main difficulty in solving 1.3 is that the traveling speed σ is unknown, which adds an additional degree of freedom. The iteration we will construct to find (σ, v) is based on the following basic observations: first, if σ is given then we can solve 1.6 to obtain the transition profile v; second, since σ is the traveling speed, a specific way to determine σ from v can be found. Thus if we let the solution operators be

$$\mathfrak{P} : \phi \to \sigma \quad \text{and} \quad \mathfrak{T} : \sigma \to \phi\,,$$

then the solution can be written abstractly as a fixed point for a system of two equations

$$(\sigma, \phi) = (\mathfrak{P}(\phi), \mathfrak{T}(\sigma))\,. \tag{1.7}$$

Remark 1. The particular form of $\mathfrak{P}$ depends on the property of ϕ and σ^*.

Since numerical simulations can only be implemented on bounded domains, we first consider equation 1.6 on a bounded domain $L = [x_l, x_r]$ with $x_l < 0$ and $x_r > 0$. Specifically, we will find (σ_*^L, ϕ^L) that satisfy

$$\begin{aligned} &-\sigma_*^L\partial_x\phi^L = \partial_{xx}\phi^L + f[\phi^L]\,, \\ &\phi^L(x_l) = 1\,, \quad \phi^L(x_r) = 0\,, \quad \phi^L(0) = \epsilon\,. \end{aligned} \tag{1.8}$$

The traveling wave solution (σ^*, v^*) to 1.6 on $\mathbb{R}$ is then recovered in the limit $x_l \to -\infty, x_r \to +\infty$ as in [19]. Here the introduction of ϵ in 1.9 becomes twofold: it provides us with an additional condition to determine σ and it avoids the translational invariance when $x_i \to \pm\infty$, $i = l, r$. If we assume $\sigma_*^L = \mathfrak{P}(\phi^L)$, $\phi^L = \mathfrak{T}(\sigma_*^L)$, then σ_*^L is a fixed point of $\sigma_*^L = \mathfrak{P}\mathfrak{T}(\sigma_*^L)$. However, the operator $\mathfrak{P}\mathfrak{T}$ is stiff. Therefore we need to use certain relaxation.

There are various possible ways to introduce relaxation to 1.8. In this paper, we will use relaxation for v. More precisely, we consider

$$\begin{aligned} \partial_t v^L - \sigma \partial_x v^L &= \partial_{xx} v^L + f[v^L]\,, \\ \sigma^L(t) &= \mathfrak{P}(v^L(t))\,, \\ v^L(x,t)|_{t=0} &= v_0(x)\,, \\ v^L(x_l) = 1\,, \quad v^L(x_r) &= 0\,, \end{aligned} \tag{1.9}$$

where $v_0(x)$ is a given initial profile and specific forms of $\mathfrak{P}$ will be determined in section 2. The traveling front of 1.2 can then be recovered if the solution of 1.9 converges to a steady state (v_*^L, σ_*^L) as $t \to \infty$. If 1.9 diverges, this suggests either there exist unstable traveling waves which is not a long time attraction for the evolution problem or there is no traveling wave.

Remark 2. The reason we use relaxation for v^L instead of σ^L is as follows. The relaxation for σ^L is

$$\begin{aligned} -\sigma^L \partial_x v^L &= \partial_{xx} v^L + f[v^L]\,, \\ \partial_t \sigma^L + \sigma^L &= \mathfrak{P}(v^L)\,, \\ v(x_l) = 1\,, \qquad v(x_r) &= 0\,. \end{aligned} \tag{1.10}$$

There are three difficulties about 1.10: first, for some σ^L the equation for v^L in 1.10 may not have a solution; second, a small change in σ^L can cause a big change in v^L, which indicates the stiffness of the mapping $v^L = \mathfrak{T}(\sigma^L)$; third, even if after some iterations σ^L converges to σ_*^L, the boundary value problem

$$-\sigma_*^L \partial_x v^L = \partial_{xx} v^L + f[v^L]\,, \qquad v(x_l) = 1\,, \qquad v(x_r) = 0$$

is sensitive to the boundary conditions. This is easy to see from the translation invariance of $L = \infty$, i.e. when $L = \infty$, v^L is not unique. Accordingly, when L is large, a very small perturbation at the value of $v(x_l)$ or $v(x_r)$ can induce a big change in v^L. Thus $v^L(0) = \epsilon$ is not guaranteed.

The advantages of our method are in the following aspects:

- The idea is extremely simple and general, it can not only apply to one single equation that exhibits traveling wave solutions, but also to systems of several equations.
- In the whole space case where $x_l = -\infty$ and $x_r = \infty$ in 1.9, the solution $u(x,t)$ of the original time evolution equation 1.2 can be precisely recovered from the solution to the relaxation equation 1.9 by the simple relation $u(x,t) = v(x - \int_0^t \sigma(\tau)\,d\tau, t)$. In a finite computational domain, $v(x - \int_0^t \sigma(\tau)\,d\tau, t)$ satisfies 1.2 with a finite moving boundary. Although this does not exactly recover $u(x,t)$ on $\mathbb{R}$, it gives approximations to $u(x,t)$ when the finite moving interval is chosen to be large enough. Therefore, by $u(x,t) \approx v(x - \int_0^t \sigma(\tau)\,d\tau, t)$, it is possible to tell whether the long time behavior of $u(x,t)$ is a traveling wave, pulsating front (as in the nonlocal Fisher-KPP example with kernel 2.20) or some other patterns.
- The computational domain is fixed, which reduces much computational cost. Though we only focus on one dimensional traveling wave simulations in the present work, this cost reduction can be significant when the convergence rate to traveling waves is slow. The extension to higher dimensions will be our future subject and we expect that this advantage will become more important.

- We can get the traveling speed automatically, which is a very important variable in reality. In practice, biologists can measure this speed by experiments.

Compared with [24, 26], there are several main differences with the scheme we propose here: *first*, the Newton iterations may not converge, especially when the solution to 1.8 is not unique or the system has no traveling wave solutions. Similar problem arises for the scheme proposed in [19]. If the Newton iteration diverges, it is not clear whether this is because there exists no traveling wave or because of the iteration itself. Whereas for the new relaxation method we propose here, certain convergence to the traveling wave solution can be proved analytically. The proof here is for the bistable case on the whole real line. It shows in long time solutions of 1.9 will converge to the traveling wave solution 1.8 for $x_l = -\infty, x_r = +\infty$. For more general cases, the proof suggests that if the solution u to the original equation 1.2 converges fast enough (in a certain sense) to a monotone traveling wave, then one can expect the convergence of 1.9 to 1.8. In addition, nonuniqueness of the traveling waves will not affect the convergence. Second, as mentioned above, our scheme enables us to see the time evolution of u, the solution to 1.2. This gives a clear picture of the propagation of the front that can be observed in physical or biological experiments. One particularly interesting phenomenon is when the long time attractor is a pulsating front instead of a traveling wave such as for the nonlocal Fisher-KPP equation. Our relaxation method can capture the periodic evolution of σ in this case. Third, we can treat more general boundary conditions. Depending on different applications, Neumann or mixed boundary conditions can also be used. Fourth, our relaxation method for v^L can only capture traveling waves that are long time attractors which is more physical relevant. For unstable traveling waves, we have to use Newton iteration for the system 1.8 as in [24, 26] or the method proposed in [19].

Different equations and systems give different forms for the solution operator $\mathfrak{P}$. In this paper we present several examples to verify the efficiency of this idea. This paper is laid out as follows. In section 2 we consider a single reaction diffusion equation 1.3. We first explain in details how to determine $\mathfrak{P}$. Next for the bistable case on $\mathbb{R}$, we prove the global well-posedness of 1.9 and justify the convergence of its solution to the desired traveling wave solution. Then we illustrate the details of the discretizations and present the numerical results of the Allen-Cahn model, the local and nonlocal Fisher/KPP equation. In section 3, we discuss the way to determine $\mathfrak{P}$ for a system of two reaction diffusion equations. Both variables in this system exhibit transit profile from one steady state to another. In section 4, we explore a hyperbolic Keller-Segel system proposed in [9] which has traveling plateau solutions and exhibits branching instabilities. Finally we conclude in section 5.

2. The reaction diffusion equation.

In this section we study scalar reaction diffusion equations. We will define the operator $\mathfrak{P}$, state the convergence of equation 1.9 to 1.8 for the bistable case as $t \to \infty$ for $x_l = -\infty$, $x_r = \infty$, and show the numerical results.

2.1. The definitions of $\mathfrak{P}$.

In this part we define the operator $\mathfrak{P}(\cdot)$ which can guarantee the additional condition $v_*^L(0) = \epsilon$ in 1.8. For the classical Fisher/KPP and nonlocal Fisher/KPP type of reaction terms, the well-posedness of 1.8 and the convergence of its solution (σ_*^L, v_*^L) to the traveling wave solution of 1.2 when $x_r, x_l \to \pm\infty$ have been proved in [1, 4, 5].

To simulate the traveling wave solutions we solve the system

$$\begin{aligned} \partial_t v^L - \sigma^L \partial_x v^L &= \partial_{xx} v^L + f[v^L]\,, \\ \sigma^L &= \mathfrak{P}(v^L)\,, \\ v^L(x_l,t) = 1\,, &\qquad v^L(x_r,t) = 0\,, \end{aligned} \tag{2.1}$$

where we define $\mathfrak{P}$ as

$$\sigma^L = \mathfrak{P}(v) = \begin{cases} \mathfrak{P}_r(v) = \frac{1}{\epsilon}\Big(\partial_x v^L|_0^{x_r} + \int_0^{x_r} v^L f[v^L]\Big), & \sigma_*^L > 0\,, \\ \mathfrak{P}_l(v) = \frac{1}{1-\epsilon}\Big(\partial_x v^L|_{x_l}^{0} + \int_{x_l}^{0} v^L f[v^L]\Big), & \sigma_*^L < 0\,. \end{cases} \tag{2.2}$$

Here σ_*^L is the traveling wave speed as in 1.8, which is unknown apriori. If the sign of σ_*^L can not be determined apriori, to achieve convergence, numerically we need to try both $\mathfrak{P}_r$, $\mathfrak{P}_l$. However, in most problems under consideration, the sign of σ_*^L is easy to see by looking at the propagation direction of the original time evolutionary equation. Moreover, if $\sigma_*^L = 0$, both $\mathfrak{P}_r$ and $\mathfrak{P}_l$ can achieve convergence, as has been proved for the bistable case in the Appendix.

By the definition in 2.2, we can formally argue that if $(\sigma^L(t),\, v^L(x,t))$ in 2.1 converges to the steady state $(\sigma_\infty^L,\, v_\infty^L(x))$ as $t \to \infty$ then $v_\infty^L(0) = \epsilon$. Then $(\sigma_\infty^L,\, v_\infty^L)$ is a solution to 1.8. By the uniqueness $(\sigma_\infty^L,\, v_\infty^L) = (\sigma_*^L,\, v_*^L)$. Indeed, the steady state of the system 2.1 satisfies

$$-\sigma_\infty^L \partial_x v_\infty^L = \partial_{xx} v_\infty^L + f[v^L]\,, \qquad v_\infty^L(x_l) = 1\,, \qquad v_\infty^L(x_r) = 0\,. \tag{2.3}$$

For the case where $\sigma_\infty^L > 0$, we integrate the equation in 2.3 from 0 to x_r to obtain

$$\sigma_\infty^L = \frac{\partial_x v_\infty^L|_0^{x_r} + \int_0^{x_r} f[v_\infty^L]}{v_\infty^L(0)}\,.$$

Comparing with the definition of σ^L in 2.1, we have $v_\infty^L(0) = \epsilon$ provided $\partial_x v_\infty^L|_0^{x_r} + \int_0^{x_r} v_\infty^L f[v_\infty^L] \neq 0$.

We remark that in 2.2 the different choices of $\mathfrak{P}$ for different signs of σ_*^L are necessary. Here we give some formal explanation. The rigorous justification over the whole space $\mathbb{R}$ is in Appendix B. From the numerical computation it appears that for certain initial data solutions of 2.1 will converge *monotonically* in time to its steady state. For this kind of solutions, if we define $\mathfrak{P}$ as $\mathfrak{P}_r$ and integrate the equation for v^L in 2.1 from 0 to x_r, then we get

$$\partial_t \int_0^L v^L \,\mathrm{d}x + v^L(0,t)\sigma^L = \partial_x v^L|_0^{x_r} + \int_0^{x_r} f[v^L] = \epsilon\,\sigma^L\,.$$

Therefore,

$$\partial_t \int_0^L v^L \,\mathrm{d}x = (\epsilon - v^L(0,t))\sigma^L\,. \tag{2.4}$$

If $\sigma^L > 0$ and we start from $v^L(x,0) < v_*^L$, so that $v^L(0,0) < \epsilon$, then 2.4 shows $\partial_t \int_0^L v^L \,\mathrm{d}x > 0$. If v^L changes monotonically in time, then the sign of $\partial_t \int_0^L v^L \,\mathrm{d}x$ is the same as $\partial_t v^L(0,0)$. Therefore $\partial_t v^L(0,0) > 0$ and $v^L(0,t)$ gets closer to ϵ after a short time. However, if we define $\mathfrak{P}$ as $\mathfrak{P}_l$, similar calculations but integrating from x_l to 0 will give

$$\partial_t \int_{x_l}^0 v^L \,\mathrm{d}x = -(\epsilon - v^L(0,t))\,\sigma^L\,. \tag{2.5}$$

In this case, under the same assumption that v^L changes monotonically with time, the conditions $\sigma^L > 0$ and $v^L(0,0) < \epsilon$ suggest $\partial_t v^L(0,0) < 0$. Thus $v^L(0,t)$ becomes even further away from ϵ and the scheme will not converge to v_*^L.

2.2. **Convergence proof for $L = \infty$.** In this part, for the bistable case, we present several propositions to show that 2.1 will converge to the steady state equation 1.8 as $t \to \infty$. The detailed proofs are given in the Appendix. The results here are for the whole real line, which on one hand serves as a clue to the case when L is big. On the other hand, considering the convergence over $\mathbb{R}$ is meaningful for its own sake, because although for computational purposes one needs to be restricted to a bounded domain, the real traveling wave is indeed defined on the whole space $\mathbb{R}$.

The convergence on a bounded domain is still unclear to us due to the complication of the boundary effect. In fact for a fixed domain, long time existence of 2.1 can be broken down for certain initial data. However, we believe this is not an essential feature of the scheme but it is related to the choice of the computational domain.

The nonlinear reaction term $f[v]$ for the bistable case satisfies the following assumptions:

$\mathcal{A}1$. $f[v]$ depends locally on v which is then denoted as $f(v)$;

$\mathcal{A}2$. $f(\cdot) \in C^1([0,1])$;

$\mathcal{A}3$. there exists some $\alpha_0 \in (0,1)$ such that

$$f(0) = f(1) = 0\,, \quad f'(0) < 0, \quad f'(1) < 0\,,$$
$$f(x) < 0 \text{ on } (0,\alpha_0)\,, \quad f(x) > 0 \text{ on } (\alpha_0, 1)\,.$$

It is known from [23] that for the bistable case there exists only one traveling front (up to a translation) with a unique traveling speed. Denote this traveling speed as σ^*. According to [23], the sign of σ^* is the same to the sign of $\int_0^1 f(x)\,\mathrm{d}x$. Here we consider the case when $\sigma^* \geq 0$. The case $\sigma^* < 0$ can be treated in a similar way.

Since it is known that $\partial_x \phi(+\infty) = 0$ for the bistable case where ϕ is the traveling front, the operator $\mathfrak{P}$ in 1.7 in this case can be given by

$$\sigma = \mathfrak{P}(\phi) = \tfrac{1}{\epsilon}\left(-\partial_x\phi(0) + \int_0^\infty f(\phi)\,\mathrm{d}x\right),$$

Hence, when $\sigma^* \geq 0$, we consider the system 2.1 for $x_l = -\infty$ and $x_r = \infty$ that has the form

$$\begin{aligned} \partial_t v - \sigma\partial_x v &= \partial_{xx} v + f(v)\,, \\ \sigma &= \tfrac{1}{\epsilon}\left(-\partial_x v(0,t) + \int_0^\infty f(v)\,\mathrm{d}x\right), \\ v(-\infty,t) &= 1\,, \qquad v(\infty,t) = 0\,, \\ v|_{t=0} &= v_0(x)\,. \end{aligned} \tag{2.6}$$

The constant ϵ is a fixed number throughout this section. The main results of this section are the well-posedness and long-time behavior of 2.6. Specifically, we will show the following three propositions:

Proposition 1 (well-posedness)**.** *Suppose f satisfies $\mathcal{A}1-\mathcal{A}3$ and the initial datum $v_0(x) \in C^1(\mathbb{R})$ satisfies A.12. Then system 2.6 has a unique solution (σ, v) for all $t > 0$. Furthermore, σ is uniformly bounded for all t.*

Proposition 2 (long-time behavior for $\sigma^* > 0$)**.** *Suppose f satisfies $\mathcal{A}1-\mathcal{A}3$ and $\int_0^1 f(x)\,\mathrm{d}x > 0$. Let (σ, v) be the solution to 2.6 with the initial datum $v_0(x)$ satisfying A.12. Then*

$$\lim_{t\to\infty} v(x,t) = \phi(x)\,, \qquad \lim_{t\to\infty} \sigma(x,t) = \sigma^*\,,$$

where σ^* and ϕ are defined in (A.6) with $\sigma^* > 0$.

Proposition 3 (long-time behavior for $\sigma^* = 0$)**.** *Suppose f satisfies $\mathcal{A}1-\mathcal{A}3$ and $\int_0^1 f(x)\,\mathrm{d}x = 0$. Let (σ, v) be the solution to 2.6 with the initial datum $v_0(x)$ satisfying A.12. Then there exists a constant a_0 depending on v_0 such that*

$$\lim_{t\to\infty} v(x,t) = \phi(x+a_0)\,, \qquad \lim_{t\to\infty} \sigma(x,t) = \sigma^* = 0\,,$$

where $(\sigma^*, \phi) = (0, \phi)$ is the solution to (A.6).

Details of the proofs of the above propositions are given in Appendix A.

2.3. **Details of the scheme.** In this part we give the details of the scheme for the case $\sigma_*^L > 0$. The discretizations are similar for $\sigma_*^L < 0$. The main purpose of this paper is to illustrate the efficiency of system 2.6 for finding traveling wave solutions, therefore, only first order numerical discretizations are tested. Any higher order numerical methods are applicable.

Discretizations: We use a uniform mesh

$$\Delta x = -\frac{x_l}{M_1} = \frac{x_r}{M_r}, \qquad x_j = j\Delta x, \quad \text{for } j = -M_l, \cdots, 0, 1, \cdots, M_r\,.$$

Let Δt be the time step and v^n, σ^n are the approximations of v^L and σ^L at the nth time step respectively. We discretize 2.1 by upwind finite difference method:

$$\begin{cases} \frac{v_j^{n+1}-v_j^n}{\Delta t} = \frac{v_{j+1}^{n+1}-2v_j^{n+1}+v_{j-1}^{n+1}}{(\Delta x)^2} + \sigma^n D_j v^n + (f[v^n])_j\,, \text{for } j = -M_l+1, \cdots, M_r-1\,. \\ v_{-M_l}^n = 1\,, \qquad v_{M_r}^n = 0\,, \\ \sigma^{n+1} = \frac{1}{\epsilon}\left(\frac{v_{M_r}^{n+1}-v_{M_r-1}^{n+1}}{\Delta x} - \frac{v_0^{n+1}-v_{-1}^{n+1}}{\Delta x} + \sum_{j=0}^{M_r-1}(f[v^n])_j \Delta x\right)\,. \end{cases} \tag{2.7}$$

Here D_j represents the first order upwind discretization such that

$$D_j v^n = \begin{cases} \frac{v_{j+1}^n - v_j^n}{\Delta x}\,, & \text{for } \sigma^n > 0\,, \\ \frac{v_j^n - v_{j-1}^n}{\Delta x}\,, & \text{for } \sigma^n < 0\,. \end{cases} \tag{2.8}$$

The convergence at zero: The specific discretization of σ^{n+1} in 2.7 is to make sure of the convergence at $x = 0$. Now we show that $v_0^L = \epsilon$ at the discrete level provided v^L converges to a steady state. Assume v^L has arrived at its steady state, i.e. $\frac{v_j^{n+1}-v_j^n}{\Delta t} = 0$, then σ^L also becomes a constant such that $\sigma^{n+1} = \sigma^n = \sigma_*^L > 0$. We multiply the equation for v^L in 2.7 by Δx and sum up over $j = 0, \cdots, M_r - 1$. By noting that $v_{M_r}^n = 0$, one gets

$$\frac{v_{M_r}^n - v_{M_r-1}^n}{\Delta x} - \frac{v_0^n - v_{-1}^n}{\Delta x} - \sigma^n v_0^n + \Delta x \sum \big(f(v^n)\big)_j = 0\,. \tag{2.9}$$

Comparing the equation for σ^{n+1} in 2.7 with 2.9, we have $v_0^n = \epsilon$. This formally indicates the steady state of 2.7 is an approximation of 1.8 on the computational

domain $[x_l, x_r]$ at the discrete level.

The constraint $v \geq 0$: Note that the positivity of the solution to the traveling front equation 1.8 is not guaranteed by the equation. In fact, depending on the choice of $f[\cdot]$, it is possible for the solution to the elliptic equation 1.8 to attain negative values. However, concerning the physical or biological background, we always want to have positive solutions. In the case when f has a particular form such that $f[v] = vg[v]$ for some g (possibly depending on v in a nonlocal form), one way to modify the reaction term is to replace $f[v^L]$ by

$$f_f[v^L] = v^L g[v^L] = \begin{cases} v^L g[v^L], & \text{for } v^L \geq 0, \\ 0, & \text{for } v^L < 0, \end{cases} \tag{2.10}$$

Then the maximum principle applied to elliptic equations can guarantee the positivity of the solution [5, 4].

Here instead we do not need to make such a modification. This is because we are only concerned with stable steady states which can be achieved as long-time profiles of solutions to the parabolic equation 1.9. More specifically, assume that $f[v] = vg[v]$ and $g[v]$ is bounded for bounded v. Then the maximum principle for parabolic equations shows that v stays nonnegative as long as it is bounded [17].

Thus if we assume that $v(x,t)$ converges to the steady state solution as $t \to \infty$, then as the limit of nonnegative functions, the solution to the steady state equation is also nonnegative.

2.4. **The numerical results.** To show the performance of our scheme, three types of $f[u]$ are tested: Allen-Cahn model, Fisher/KPP equation, and the nonlocal Fisher equation. These three models exhibit traveling front solutions with different behaviors. The first two equations have already been well studied both analytically and numerically [23]. It is known [23] that the Allen-Cahn equation has a unique traveling speed, whose sign depends on the choice of the parameter α in f, while the Fisher/KPP equation has a range of possible traveling speeds. The nonlocal Fisher equation has more abundant and interesting behaviors, which can exhibit pattern formation in a single equation.

In all the numerical examples, we use $\epsilon = 0.5$. The computational domains are $[-10, 10]$, $[-20, 20]$, $[-40, 40]$ which are denoted by $L = 20, 40, 80$ respectively. The stopping criterion for the calculation is

$$\|v^{n+1} - v^n\|_\infty = \max_j\{|v_j^{n+1} - v_j^n|\} < 10^{-5}. \tag{2.11}$$

All the displayed pictures have two subplots: the top ones depict the limiting profiles of v^L when they converge while the bottom ones show the time evolution of $\sigma(t)$.

The Allen-Cahn model. The one dimensional Allen-Cahn equation is

$$\partial_t u = \partial_{xx} u + u(1-u)(u-\alpha), \tag{2.12}$$

with $\alpha \in (0,1)$. As discussed in [23], the steady state $u \equiv 1$, $u \equiv 0$ are conditionally stable while the other steady state $u \equiv \alpha$ is unconditionally unstable. Additionally, we have

Theorem 2.1 ([23]). *For any $\alpha \in (0,1)$, Allen-Cahn equation 2.12 has a unique traveling wave solution (σ^*, u) such that*

$$\sigma^* > 0, \quad \textit{for } 0 < \alpha < \tfrac{1}{2}; \quad \sigma^* < 0, \quad \textit{for } \tfrac{1}{2} < \alpha < 1; \quad \sigma^* = 0, \quad \textit{for } \alpha = \tfrac{1}{2}.$$

This example enables us to verify the strategy of choosing $\mathfrak{P}_l$, $\mathfrak{P}_r$ and Proposition 3. When $\alpha < 0.5$, the convergence can be achieved using $\mathfrak{P}_r$. When $\alpha > 0.5$, we use $\mathfrak{P}_l$. When $\alpha = 0.5$, both $\mathfrak{P}_l, \mathfrak{P}_r$ can be used to find $\sigma_*^L = 0$, but $v^L(0) = \epsilon$ is not necessarily satisfied.

Although the definition of σ requires v^L to be continuous at 0, at the discrete level, since we are using one-sided finite difference $\frac{v_0^{n+1} - v_{-1}^{n+1}}{\Delta x}$ as in 2.7, we can start from

$$v(x) = \begin{cases} 1, & x \in [x_l, 0], \\ 0, & x \in (0, x_r]. \end{cases}$$

The numerical results for different α are presented in Figure 1. The shapes of v^L do not change much when L increases and the traveling speed σ^L does converge to some constant. Moreover, the resulting σ^L's for $\alpha = 0.3, 0.5, 0.8$ verify Theorem 2.1.

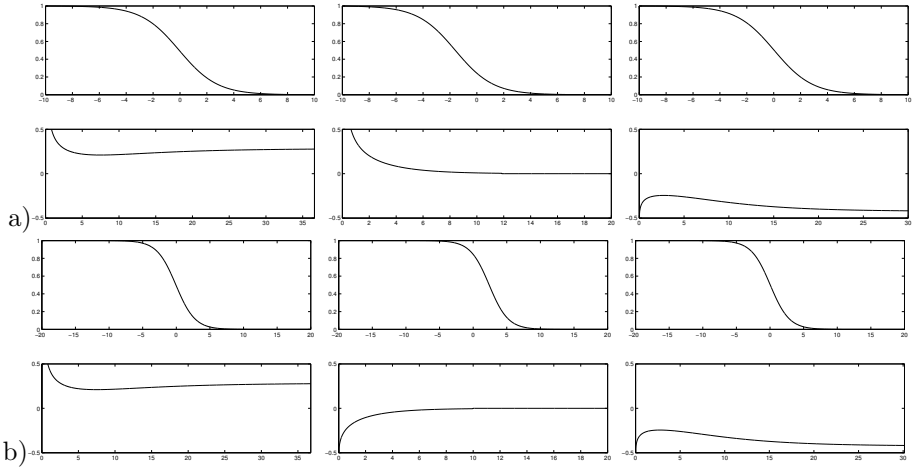

FIGURE 1. The traveling wave solution v^L and σ^L for Allen-Cahn model with different $\alpha = 0.3$ (left), $\alpha = 0.5$ (middle) and $\alpha = 0.8$ (right). In each figure, the top subplot is the shapes of v^L when they have arrived at convergence while the bottom subplot shows the convergence of σ^L. a) The results for $L = 20$; b) $L = 40$.

Fisher/KPP equation. The Fisher/KPP equation is as follows:

$$\partial_t u = \partial_{xx} u + u(1 - u). \tag{2.13}$$

It is well known that the traveling speed for Fisher/KPP is not unique [15]. Theoretically, 2.13 has a traveling wave solution $0 \le v \le 1$ for any speed $\sigma^* \ge 2$. However only the traveling wave with speed $\sigma^* = 2$ is dynamically stable with a large basin of attraction and can be obtained from evolution equations.

Consider the equation

$$\begin{aligned} &-\sigma_*^L \partial_x v_*^L = \partial_{xx} v_*^L + v_*^L(1 - v_*^L), \qquad 0 \le v_*^L \le 1, \\ &v_*^L(x_l) = 1, \quad v_*^L(x_r) = 0, \quad v_*^L(0) = \epsilon. \end{aligned} \tag{2.14}$$

As discussed in [4], the solution of 2.14 will give us the critical speed $\sigma^* = 2$ when $x_l, x_r \to \pm\infty$. For L finite, as part of the solution to the above equation, σ_*^L is less

than 2 and positive. Therefore we use $\mathfrak{P}_r$ here. In the subsequent part, we test numerically the convergence of our scheme and the effects of different choices of ϵ and computational domains.

- In order to check the convergence of the scheme, we fix $[x_l, x_r] = [-20, 20]$, $\epsilon = 0.5$, and choose an initial condition that is smooth, decays exponentially with a sufficiently large decay rate, and satisfies the boundary conditions in 2.1:

$$v^L(x,0) = \begin{cases} 1\,, & x \in [-20,-5]\,, \\ \frac{e^{-5(x+5)} - e^{-5(x_r+5)}}{1-e^{-5(x_r+5)}}\,, & x \in [-5,20]\,. \end{cases}$$

  In Table 1, the numerical results of different $\Delta x, \Delta t$ are compared with the "exact" solution (σ^L, v^L), which is calculated by the very fine mesh $\Delta x = 1/1280, \Delta t = 1/1280$. Here

$$\|E_v(x,i)\|_\infty = \max_{j=-M_l,\cdots,M_r} |v_j^{L[i/\Delta t]} - v^L(x_j,i)|\,, \quad \text{for } i = 10, 20\,,$$
$$\|E_\sigma\|_\infty = \max_{n=1,\cdots,[20/\Delta t]} |\sigma^n - \sigma^L(n\Delta t)|\,,$$

  where $[i/\Delta t]$ denotes the integer part of $i/\Delta t$. First order convergence in both space and time can be easily observed.

Δx	Δt	$\|E_v(x,10)\|_\infty$	$\|E_v(x,20)\|_\infty$	$\|E_\sigma\|_\infty$
1/40	1/1280	$2.174 * 10^{-3}$	$2.687 * 10^{-3}$	$2.188 * 10^{-2}$
1/80	1/1280	$1.049 * 10^{-3}$	$1.295 * 10^{-3}$	$1.059 * 10^{-2}$
1/160	1/1280	$4.891 * 10^{-4}$	$6.033 * 10^{-4}$	$5.061 * 10^{-3}$
1/320	1/1280	$2.095 * 10^{-4}$	$2.583 * 10^{-4}$	$2.169 * 10^{-3}$
1/80	1/80	$1.022 * 10^{-3}$	$1.307 * 10^{-3}$	$1.010 * 10^{-2}$
1/160	1/160	$4.769 * 10^{-4}$	$6.099 * 10^{-4}$	$5.136 * 10^{-3}$
1/320	1/320	$2.045 * 10^{-3}$	$2.614 * 10^{-3}$	$2.202 * 10^{-3}$

TABLE 1. The space and time convergence of our scheme for the Fisher/KPP equation.

- The numerical results with $\Delta x = \Delta t = 1/320$ are presented in Figure 3 with different choices of ϵ such as $\epsilon = 0.01, 0.1, 0.5,$. Although the evolution of σ^L depends on ϵ, eventually they all converge to the same constant which is independent of ϵ. Moreover, the transit profiles of v^L are the same up to a spatial shift. Since 2.13 is independent of ϵ, the original solution u^L recovered from v^L should also be independent of ϵ. The sameness of u^L in Figure 3 illustrates the advantage claimed in the introduction that we can recover the solution of the original Fisher/KPP equation at any time $t > 0$.
- The different values of σ^L are shown in Table 2 for different choices of Δx and L. Figure 4 shows that numerically, σ^L depends on Δx and has first order convergence. The results of $L = 40$ and $L = 80$ in Table 2 indicate that σ^L does not change much when L big enough. However, by comparing σ^L for $L = 20$ and $L = 40$, one can see that σ^L is closer to 2 for larger L's.

Nonlocal Fisher/KPP equation. The nonlocal Fisher/KPP equation is

$$\partial_t u = \partial_{xx} u + \mu u(1 - \psi \star u)\,, \tag{2.15}$$

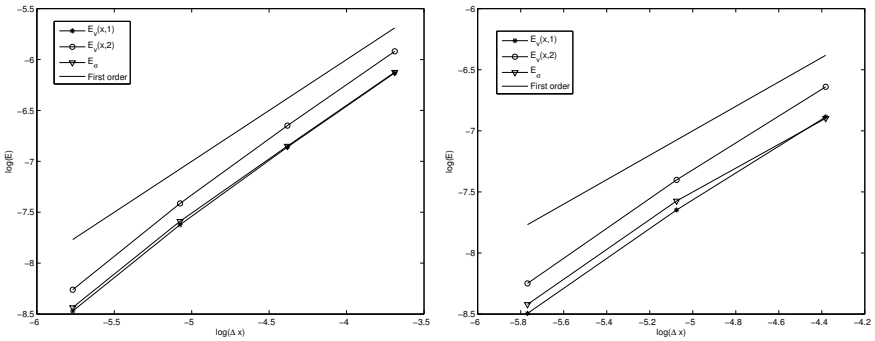

FIGURE 2. The log-log plot of the errors in Table 1. The log of $E_v(x,1)$, $E_v(x,2)$, E_σ with respect to the log of Δx are plotted by stars, circles and triangles respectively. Left: $\Delta t = 1/1280$; right: $\Delta t = \Delta x$. The first order convergence with respect to Δx can be seen clearly.

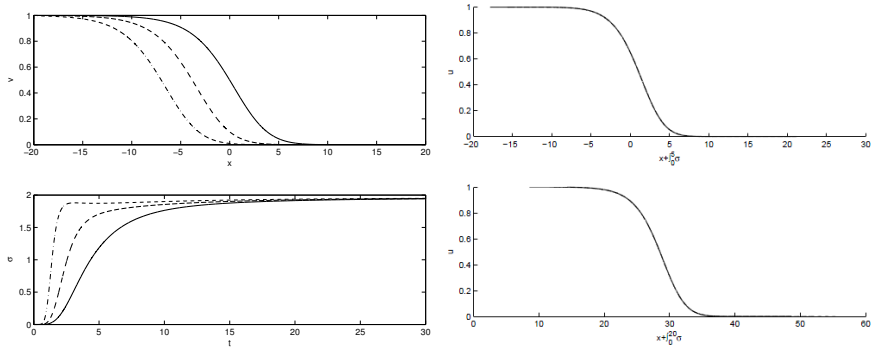

FIGURE 3. The effect of ϵ in the simulation for Fisher/KPP equation. The dash dotted, dashed and solid lines are the numerical results with $\epsilon = 0.01, 0.1, 0.5$ respectively. Left: the converged profile of v^L (top) and the evolution of σ^L (bottom). Right: the space shift of $v^L(x,5)$ to $u^L(x + \int_0^5 \sigma^L(\tau)\,d\tau, t)$ (top) and $v^L(x,20)$ to $u^L(x + \int_0^{20} \sigma^L(\tau)\,d\tau, t)$ (bottom). The results of $\epsilon = 0.01, 0.1, 0.5$ are so close to each other that all three lines overlap. Here we use $[x_l, x_r] = [-20, 20]$, $\Delta x = \Delta t = 1/320$.

with $\psi(x)$ the convolution kernel such that

$$\psi \star u(x) = \int_{\mathbb{R}^d} u(x-y)\psi(y)\,\mathrm{d}y\,. \tag{2.16}$$

The boundary conditions are

$$u(-\infty, t) = 1\,, \qquad u(\infty, t) = 0\,.$$

	$L=20$		$L=40$		$L=80$	
Δx	$\lvert v^L(0)-\epsilon\rvert$	σ^L	$\lvert v^L(0)-\epsilon\rvert$	σ^L	$\lvert v^L(0)-\epsilon\rvert$	σ^L
0.04	$1.9341*10^{-3}$	1.8143	$2.6999*10^{-3}$	1.8715	$2.6999*10^{-3}$	1.8715
0.02	$1.92916*10^{-3}$	1.8286	$2.7003*10^{-3}$	1.8898	$2.7003*10^{-3}$	1.8898
0.01	$1.92624*10^{-3}$	1.8358	$2.7019*10^{-3}$	1.8989	$2.7019*10^{-3}$	1.8989
0.005	$1.9246*10^{-3}$	1.8393	$2.7005*10^{-3}$	1.9035	$2.7005*10^{-3}$	1.9035
0.0025	$1.9239*10^{-3}$	1.8411	$2.6998*10^{-3}$	1.9058	$2.6998*10^{-3}$	1.9058

TABLE 2. The obtained σ^L with $\Delta t = 0.01$ and different $L, \Delta x$.

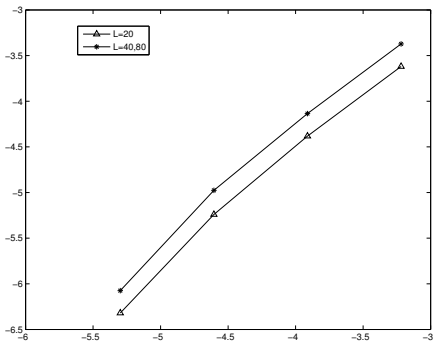

FIGURE 4. The log-log plot of the difference of the obtained $\sigma^L(\Delta x)$ to the referred σ^L with respect to Δx. The x-axis is $\log \Delta x$ while the y-axis is $\log(\sigma^L - \sigma^L(\Delta x))$. For $L = 20, 40, 80$, σ^L have first order convergence with respect to Δx. Moreover, σ^L do not change much when L big enough.

The function v^L is only defined in $[x_l, x_r]$. In order to calculate $\psi \star v^L$, we extend v^L to $\mathbb{R}$ by

$$v(x) = \begin{cases} 1\,, & x \in (-\infty,\, x_l)\,, \\ v^L\,, & x \in [x_l, x_r]\,, \\ 0\,, & x \in [x_r,\, +\infty]\,. \end{cases} \tag{2.17}$$

In [4] the authors proved the existence of the solutions to 1.8 with $f[v] = \mu v(1 - \psi \star v)$, assuming that $\psi(x)$ satisfies

$$\psi \geq 0\,, \quad \psi(0) > 0\,, \quad \nabla\psi \in C_b(\mathbb{R}^d)\,, \quad \int_{\mathbb{R}} \psi(x)\,\mathrm{d}x = 1\,, \quad \int_{\mathbb{R}} x^2\psi(x)dx < \infty\,, \tag{2.18}$$

Then v^L converges up to a subsequence to a traveling wave solution with speed $2\sqrt{\mu}$ as $x_i \to \pm\infty$, $i = l, r$.

With our relaxation method, the numerical results of two different kernels are given in the subsequent part. The equilibrium state $u \equiv 1$ is always linearly stable for the first kernel but not for the second kernel. Although the relaxation method can not find the unstable traveling wave solution, we can still see the time evolution of the solution.

Example 1. The Gaussian probability density where

$$\psi = \frac{1}{\sqrt{2\pi\mu^2}} \exp\Big(-\frac{x^2}{2\mu^2}\Big). \tag{2.19}$$

Since $\hat{\psi}(\xi) = \exp(-\xi^2\mu^2/2) > 0$ for all $\xi \in \mathbb{R}$, it is proved in [4] that in this case the equilibrium state $u \equiv 1$ is always linearly stable. In Figure 5, using the relaxation method, we present the shapes of v^L and the convergence of σ^n with respect to t. Here considering the accuracy when $\mu = 200$, we use $\Delta t = \Delta x = 1/400$. Numerically, the shapes of v^L do not change when we increase L and the bigger μ is, the smaller $\Delta t, \Delta x$ are required. It is obvious that the traveling wave solution connects two steady states 1 and 0, which verifies the theoretical results in [4].

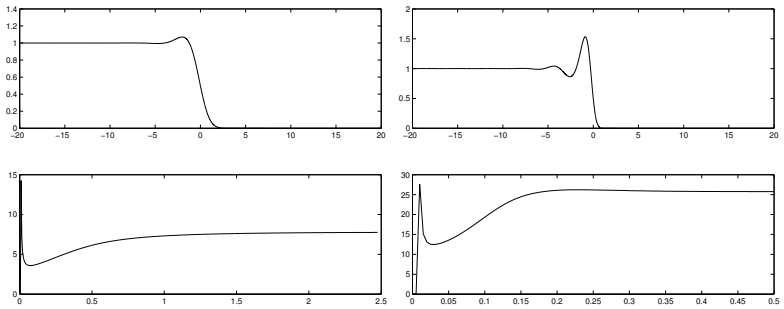

FIGURE 5. The shapes and convergence of traveling wave solution for the nonlocal Fisher/KPP equation with Gaussian kernel (2.19). With the same $\Delta t = \Delta x = 0.0025$, the results for different μ's are presented. Left: $\mu = 16$; right: $\mu = 200$.

Example 2. The second kernel ϕ is chosen as

$$\psi_a = \tfrac{1}{2}\mathbf{1}_{[-1,1]}(x). \tag{2.20}$$

In this case $\hat{\psi}(\xi) = \sin(\xi a)/(\xi a)$ which can be negative for some ξ_0. By [4], there exists $0 < \mu_c < \infty$ such that for $\mu > \mu_c$, the state $v \equiv 1$ is linearly unstable.

Numerically, when μ is small, we can find similar profiles of the traveling wave solutions and convergence of σ^L as for the Gaussian kernel. However, for μ big, this is no longer true. As shown in Figure 6, when $\mu = 200$, the relaxation method can not give the traveling waves solution as in Figure 6(c). Instead it shows some periodic pattern which is similar to the original evolution equation. This is because when μ is big, the traveling wave solution is unstable and is no longer an attraction of the system 2.1. Compared with direct simulation of time evolutionary equation, our relaxation method can not only use smaller computational domain, but also obtain the time periodicity of σ^L, which suggests that the so obtained v^L is a pulsating front [20].

3. System with two reaction diffusion equations.

The idea of the relaxation method can easily be extended to systems. In this section, we consider the renormalized form of one dimensional laminar flame equation and present the numerical scheme and performance.

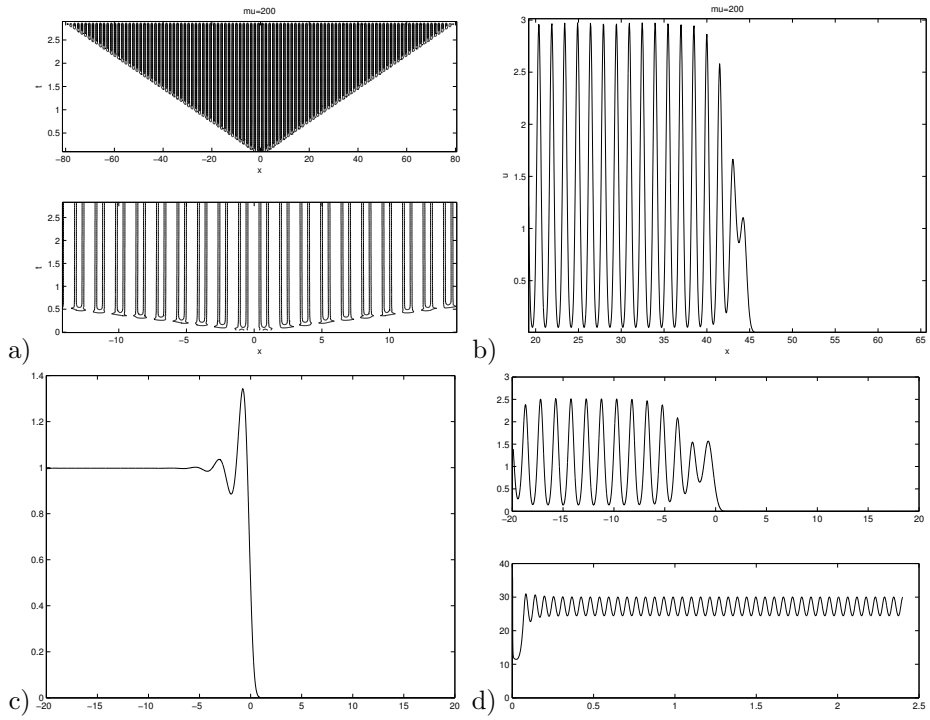

FIGURE 6. For the second kernel, the numerical results for $\mu = 200$. a):The isolines of $u(x,t)$; b): the front of v calculated by the time evolutional equation (1.2). c): the traveling wave solution obtained by the method proposed in [19]. d): the periodic behavior of $\sigma^L(t)$ by our relaxation method with $\Delta x = 0.002, \Delta t = 0.001$.

3.1. **The equations and definition of $\mathfrak{P}$.** Let T be the the temperature and Y be the species concentration. The flame propagation model with no fluid mechanics involved has the form

$$\begin{cases} \partial_t T = \partial_{xx} T + Y f[T]\,, \\ \partial_t Y = \Lambda \partial_{xx} Y - Y f[T]\,, \end{cases} \tag{3.1}$$

where Λ is a constant which is called the Lewis number [5]. The reaction term $f[T]$ satisfies [23]

$$f[0] = 0\,, \qquad f'[0] = 0\,, \qquad f'[T] > 0 \quad \text{for } T > 0$$

or as in [5]

$$f : [0,1] \to \mathbb{R}^+ \text{ is continuous, locally Lipschitz on } (\theta, 1], \text{ possibly discontinuous at } T = \theta,\ f[T] = 0\,, \text{on } [0,\theta]\,, \qquad f[T] > 0\,, \text{on } [\theta, 1] \tag{3.2}$$

Currently we only consider f locally depending on T. The boundary conditions are

$$T(-\infty) = 0\,, \quad T(\infty) = 1\,; \qquad Y(-\infty) = 1\,, \quad Y(\infty) = 0\,.$$

This model arises in combustion theory that describes the propagation of flames. It can also model bacterial colonies where T represents the density of cells and Y the consumed nutrients [6].

The traveling wave solution of (3.1) satisfies

$$\begin{cases} -\sigma^*\partial_x T^* = \partial_{xx}T^* + Y^* f[T^*]\,, \\ -\sigma^*\partial_x Y^* = \Lambda\partial_{xx}Y^* - Y^* f[T^*]\,. \end{cases} \tag{3.3}$$

Two possible $\mathfrak{P}$'s for this system can be used: one is to fix $T^*(0) = \epsilon$ and the other is $Y^*(0) = \epsilon$. Here we use $T^*(0) = \epsilon$ to avoid the transition invariance and consider a bounded domain $[x_l, x_r]$. Because the sign of σ_*^L is not known apriori, to achieve convergence, numerically we need to try both $\mathfrak{P}_r$, $\mathfrak{P}_l$. It turns out that due to the boundary condition $T(x_l) = 0$, the particular $\mathfrak{P}$ that gives the convergence is

$$\sigma^L = \mathfrak{P}(T) = -\frac{\partial_x T|_{x_l}^0 + \int_{x_l}^0 Y f[T]}{\epsilon}\,.$$

Similar as the discussions for 2.4, 2.5, here the choice of $\mathfrak{P}$ can be seen formally as follows. We are going to find the steady state of the following system:

$$\begin{cases} \partial_t T^L - \sigma^L\partial_x T^L = \partial_{xx}T^L + Y^L f[T^L]\,, & T^L(x_l) = 0\,, \quad T^L(x_r) = 1\,, \\ \partial_t Y^L - \sigma^L\partial_x Y^L = \Lambda\partial_{xx}Y^L - Y^L f[T^L]\,, & Y^L(x_l) = 1\,, \quad Y^L(x_r) = 0\,, \\ \sigma^L = -\frac{\partial_x T^L|_{x_l}^0 - \int_{x_l}^0 Y^L f[T^L]}{\epsilon}\,. \end{cases} \tag{3.4}$$

By integrating the equation of T^L from x_l to 0, we have

$$\partial_t \int_{x_l}^0 T^L = (T^L(0,t) - \epsilon)\sigma^L\,.$$

Start from $T^L(x,0)$ which is a small perturbation of T_*^L such that $T^L(0,0) < \epsilon$. If $\sigma_*^L < 0$, then it implies $\partial_t \int_{x_l}^0 T^L(x,0)\,\mathrm{d}x > 0$ at $t = 0$. Under the assumption that T^L changes monotonically with time, we have $\partial_t T^L(0,0) > 0$. Therefore $T^L(0,t)$ gets closer to ϵ after a short time as desired. The steady state of 3.4 satisfies 3.3 on $[x_l, x_r]$ and similar as the discussion for 2.1, the additional equation of σ^L in 3.4 fixes the point $T^L(0) = \epsilon$.

3.2. **Numerical results.** Numerically, we take

$$f[T] = \begin{cases} 0\,, & T < \theta\,, \\ T\,, & T \geq \theta\,, \end{cases}$$

with $\theta = 10^{-3}$, which satisfies 3.2. The introduction of θ (ignition temperature) is to avoid the cold boundary difficulty, so as to make sure that $(T(-\infty), Y(-\infty)) = (0, 1)$ is a steady state of 3.1 (cf. [3]). As proved in [5], the traveling wave solutions exist for $\theta > 0$. Figure 7 gives the numerical results for different $\Lambda = 0.1,\ 1,\ 10$. We can see that the flame shapes and σ^L converge to a negative constant, which confirms our choice of $\mathfrak{P}$.

4. **The hyperbolic Keller-Segel model.** In this section, we consider a hyperbolic Keller-Segel system which exhibits traveling plateaus.

4.1. **The system and definition of $\mathfrak{P}$.** In [9], the authors proposed a new model that describes the spreading of cells in colonies on rich media. The spreading occurs

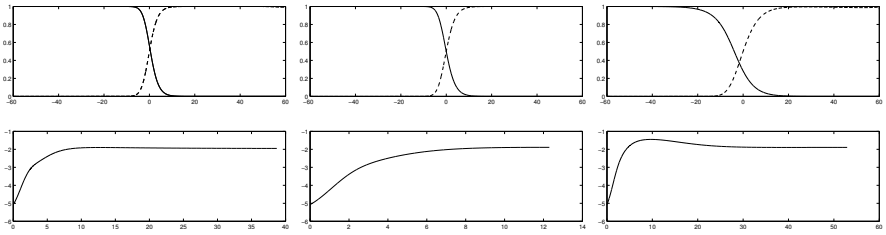

FIGURE 7. The traveling wave solution of (3.1) for different Λ. Left: $\Lambda = 0.1$, middle: $\lambda = 1$; right: $\lambda = 10$. In all the pictures, the top subplots depict the front shapes of Y, T by solid and dashed lines respectively, the bottom subplots show the convergence of σ^L.

under the effect of cellular communication through excretion of signalling molecules and exhibits complex patterns. The system is

$$\begin{cases} \partial_t \rho + \partial_x[(1-\rho)\rho\partial_x c - \rho\partial_x S] = 0, \\ -D_c\partial_{xx} c + c = \alpha_c \rho, \\ \partial_t S - D_S \partial_{xx} S = \alpha_S \rho, \end{cases} \tag{4.1}$$

which takes into account the prevention of overcrowding effect, sometimes also referred as "volume filling" effect, by $\rho(1-\rho)$ and the repellent forces $\partial_x S$. It has been proved in a recent work that this system has traveling plateau solutions under certain size conditions [22]. Here traveling plateau or traveling pulse indicate that the shape of $\rho(x)$ keeps like a plateau or pulse and moves forward.

Our goal here is to extend the relaxation method to this system to find its traveling pulse solutions. The traveling wave equation is

$$\begin{cases} -\sigma\partial_x \rho^* + \partial_x[(1-\rho^*)\rho^*\partial_x c^* - \rho\partial_x S^*] = 0\,, \\ -D_c\partial_{xx} c^* + c^* = \alpha_c \rho^*\,, \\ -\sigma\partial_x S^* - D_S\partial_{xx} S^* = \alpha_S \rho^*\,, \end{cases} \tag{4.2}$$

in which

$$\rho^* > 0, \quad \forall x \in [-l, l], \qquad \rho^* = 0, \quad \text{elsewhere}\,. \tag{4.3}$$

The boundary conditions are

$$c^*(\pm\infty) = 0\,, \qquad S^*(-\infty) = S_\infty\,, \qquad S^*(+\infty) = 0\,.$$

The quantity $S^*(x)$ is defined up to an additive constant and we have fixed it by imposing $S^*(+\infty) = 0$. This is in accordance with the fact that it represents a molecule (surfactine) excreted by the cells and diffused in the media. As discussed in [22], the Neumann boundary conditions

$$\partial_x c^*(\pm\infty) = 0\,, \qquad \partial_x S^*(-\infty) = 0\,, \qquad S^*(+\infty) = 0\,, \tag{4.4}$$

are also possible. Numerically, the Dirichlet boundary conditions are difficult to deal with, as S_∞ is not known. For the subsequent calculations, we use the Neumann boundary conditions 4.4.

We are going to solve the system

$$\begin{cases} \partial_t \rho - \sigma \partial_x \rho + \partial_x[(1-\rho)\rho \partial_x c - \rho \partial_x S] = 0\,, \\ -D_c \partial_{xx} c + c = \alpha_c \rho\,, \\ \partial_t S - \sigma \partial_x S - D_S \partial_{xx} S = \alpha_S \rho\,. \end{cases} \tag{4.5}$$

If σ is known, then starting from $(\rho(x,0), S(x,0))$ we can find the traveling wave solution by finding the steady state of 4.5. From this example we can see the advantage of the relaxation method compared to [24, 26, 19]. Since the solution to 4.2 is not unique and the steady state of 4.5 depends on the initial ρ, S, we can no longer use Newton iteration to find the traveling wave solutions.

The problem is how to find an expression for σ. This expression will serve as an additional condition to fix the front position, which is the critical point of our method. Similar as before, we use

$$\sigma = \mathfrak{P}(S) = \frac{1}{\epsilon}\big(D_S \partial_x S|_0^{x_r} + \alpha_S \int_0^{x_r} \rho \,\mathrm{d}x\big)\,. \tag{4.6}$$

Then 4.5, 4.6 form a closed system for ρ, c, S and σ. This system can be solved as follows: for given σ^0, ρ^0,

(i) Prepare the initial S^0 by solving

$$-\sigma^0 \partial_x S^0 - D_s \partial_x^2 S^0 = \alpha_S^0 \rho^0,$$

on the interval $[x_l, x_r]$ with the boundary conditions

$$\partial_x S^0(x_l) = 0\,, \qquad S^0(x_r) = 0\,;$$

(ii) Using $\sigma = \sigma^0$, solve the system 4.5 for one time step and obtain ρ^1, c^1, S^1 with the boundary conditions in 4.4. Here we use ρ^1 on the right hand side of (4.5) to update c^1 and S^1;

(iii) Update σ by 4.6 and find σ^1;

(iv) Go to step (ii) and update with $\sigma = \sigma^1$ and the initial conditions ρ^1, S^1. Do the loops until $\sigma(t), \rho(t)$ converge.

Remark 3. Prescribing ρ^0, S^0 is also a possible choice which has more biophysical meaning according to 4.1. However, depending on the initial S^0, the convergence to the traveling wave could take a long time. For convenience, We prescribe σ^0 here to prepare a S^0 that is close to the traveling wave profile initially.

4.2. **Numerical results.** The equation for ρ in 4.5 is a nonlinear hyperbolic equation that involves shocks. Therefore we need to use shock capture methods to discretize the space. Here a first order finite volume Engquist-Osher-type scheme [8] is employed.

Let the computational domain be $[-30, 30]$ and we choose the parameters as

$$\alpha_c = 1, \quad \alpha_S = 1, \quad D_c = 0.1, \quad D_S = 1.$$

The initial ρ^0, σ^0 are

$$\sigma^0 = 1\,. \qquad \rho^0 = \begin{cases} 1 - \frac{\alpha_S D_c}{\alpha_c D_S} = 0.9\,, & \text{for } x \in (-l, l)\,, \\ \rho^0 = 0\,, & \text{elsewhere.} \end{cases}$$

Numerically, we use $\epsilon = 1$ to fix the transit profile position. Different values of l are tested. When $l = 0.2, 0.3, 0.4$, the evolutions of σ and the final shape of ρ, S are plotted in Figure 8. We can see that when $l = 0.2, 0.3$, σ converges to a constant and ρ, S becomes stable. This gives us the traveling wave solution of the small

plateaus when $l = 0.2, 0.3$. Nevertheless, when $l = 0.4$, Figure 8 c) shows that the plateau splits and S_∞, σ no longer converge. These results recover the theoretical and numerical observation in [22].

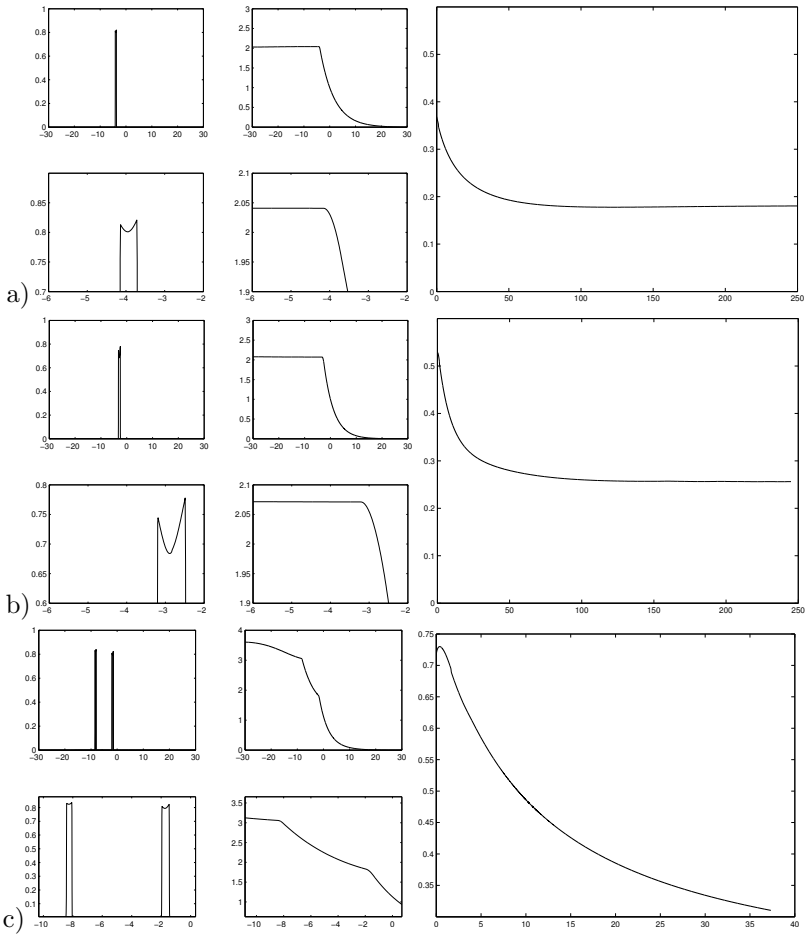

FIGURE 8. The traveling wave solution for different l, Left: The steady ρ (left) and S (right) are presented, where the bottom subplots are the zoom-in of top subplots; Right: the evolutions of σ. a)$l = 0.2$; b) $l = 0.3$; c) $l = 0.4$.

5. **Conclusion.** In this paper, we present a new method for traveling wave simulations. Traveling wave solutions are quite interesting in both theoretical and practical aspects. They are used to describe flame propagation in combustion theory, the progress of an invasive species in ecology, the formation of dentritic patterns, the calcium pulses in neuroscience and many other phenomena. The main difficulty of its simulation is that the traveling velocity is unknown. The idea of this new method is that first we fix a point in the computational domain to find an additional expression for the traveling velocity. Then by the relaxation method, we solve the combined system to get the transition profiles and the traveling velocity

simultaneously. The introduction of an additional point not only avoids the transition invariance but also gives us the expression for σ^L, which is the most interesting quantity that can be measured experimentally.

Analytically, for the scalar bistable reaction-diffusion equation, we prove that the long time behavior of this new system 2.6 converges to the traveling wave solutions.

On the numerical side, we show the implements of our scheme to various models: Allen-Cahn model, local and nonlocal Fisher/KPP equation, laminar flame equation, and a hyperbolic Keller-Segel model. These models all arise in mathematical biology or chemistry. Comparing with solving the original time evolution problem, here smaller computational domains are required and the traveling velocity can be found. Moreover, in the simulation of nonlocal Fisher/KPP equation when $u = 1$ is Turing unstable, it is hard to capture the periodic behavior of σ^L in time by solving the original time evolution equation. This periodicity however is important, since it indicates that the observed profile in the original evolution equation is a pulsating front instead of a traveling wave.

On the other hand, although the idea of fixing one point in the computational domain has already been investigated in [26, 24], they use Newton method to solve the boundary value problem directly. In the simulation of the hyperbolic Keller-Segel model, Newton iteration is not applicable when the solution is not unique or when there is no traveling wave solution. Whereas, our relaxation method can show the time evolution and is applicable independent of the uniqueness and existence of the traveling wave solution.

The idea of our method is simple and natural which can also be applied to many other equations that exhibit traveling wave solutions. The generalization to pulsating traveling fronts [2, 20] is straight forward and it is a work in progress [27]. The two dimensional cases will be our future subject.

Appendix A. Convergence Proof.

In this appendix we prove Proposition 1, 2, and 3 stated in Section 2.2. Note that by assumptions $\mathcal{A}2$ and $\mathcal{A}3$ in Section 2.2, there exists C_α such that

$$|f(x)| \le C_\alpha\, x(1-x)\,, \qquad \text{for all } x \in [0,1]\,. \tag{A.1}$$

Define the two constants:

$$\gamma_0 = \min\{|f'(0)|,\, |f'(1)|\}\,, \qquad K = \|f'(x)\|_{L^\infty(0,1)}\,. \tag{A.2}$$

We first state two results in [14] and prove a few lemmas. Proofs of Proposition 1, 2, and 3 will be at the end of this section.

Theorem A.1 ([14]). *Suppose that f satisfies $\mathcal{A}1-\mathcal{A}3$ and u is the unique solution to the equation*

$$\begin{gathered} \partial_t u = \partial_{xx} u + f(u)\,, \\ u(-\infty, t) = 1\,, \quad u(\infty, t) = 0\,, \\ u(x,0) = u_0(x)\,, \end{gathered} \tag{A.3}$$

where the initial datum $u_0(x)$ is piecewise continuous and satisfies

$$0 \le u_0(x) \le 1\,, \qquad \lim_{x\to-\infty} u_0(x) = 1\,, \qquad \lim_{x\to\infty} u_0(x) = 0\,. \tag{A.4}$$

Then $0 \le u(x,t) \le 1$ and there exists $x_0 \in \mathbb{R}$ and $K_0, \delta > 0$ independent of x such that

$$|u(x+\sigma^* t, t) - \phi(x + x_0)| \le K_0\, e^{-\delta t}\,. \tag{A.5}$$

Here (σ^*, ϕ) is the unique solution to the traveling wave equation

$$\begin{aligned} -\sigma^* \partial_x \phi &= \partial_{xx}\phi + f(\phi)\,, \\ \phi(-\infty) = 1\,, \quad \phi(\infty) &= 0\,, \quad \phi(0) = \epsilon\,, \end{aligned} \tag{A.6}$$

where $0 < \epsilon < 1$ is the fixed number as in 2.6 and ϕ is monotonically decreasing.

Define the shifted profile $\bar{u}(x,t)$ as

$$\bar{u}(x,t) = u(x + \sigma^* t, t)\,. \tag{A.7}$$

where σ^* is the traveling speed in A.6. Then $\bar{u}$ satisfies

$$\begin{aligned} \partial_t \bar{u} - \sigma^* \partial_x \bar{u} &= \partial_{xx}\bar{u} + f(\bar{u})\,, \\ \bar{u}(-\infty, t) = 1\,, \quad \bar{u}(\infty, t) &= 0\,, \\ \bar{u}(x,0) &= u_0(x)\,. \end{aligned} \tag{A.8}$$

Theorem A.1 immediately gives

Corollary 1. *Let f, u, σ^*, ϕ be the same as in Theorem A.1. Then there exists $K_1 > 0$ independent of x such that for any $t > 1$ the shifted profile $\bar{u}$ defined in A.7 satisfies*

$$|\partial_x \bar{u}(x,t) - \partial_x \phi(x + x_0)| \le K_1\, e^{-\delta t}\,, \tag{A.9}$$

where $\delta > 0$ is the same as in A.5.

Proof. The proof follows from a mild version of the interior Schauder estimates for the inhomogenous parabolic equation for $\bar{u}(x,t) - \phi(x)$. This equation has the form

$$\partial_t(\bar{u} - \phi) - \sigma^* \partial_x(\bar{u} - \phi) = \partial_{xx}(\bar{u} - \phi) + (\bar{u} - \phi) G(\bar{u}, \phi)\,,$$

where

$$G(\bar{u}, \phi) = \begin{cases} \frac{f(\bar{u}) - f(\phi)}{\bar{u} - \phi}\,, & \bar{u} \neq \phi\,, \\ f'(\bar{u})\,, & \bar{u} = \phi\,. \end{cases}$$

By A.2, G is well-defined and $|G| \le K$ on $[0,1] \times [0,1]$. Here K is defined in A.2. Then for any $t_0 > 0$, a mild version of the interior Schauder estimate (see (1.4) of [14]) gives

$$\begin{aligned} &\sup_{x \in \mathbb{R},\, t \ge t_0 + 1} |\partial_x \bar{u}(x,t) - \partial_x \phi(x + x_0)| \\ &\le C\Big(\sup_{x \in \mathbb{R},\, t \ge t_0} |(\bar{u}(x,t) - \phi(x + x_0))\, G(\bar{u}, \phi)| + \sup_{x \in \mathbb{R}} |\bar{u}(x, t_0) - \phi(x + x_0)| \Big)\,, \end{aligned}$$

for some $C > 0$ which is independent of t_0, $\bar{u}$, and ϕ. By A.5 this implies for all $t_0 > 0$,

$$\sup_{x \in \mathbb{R},\, t \ge t_0 + 1} |\partial_x \bar{u}(x,t) - \partial_x \phi(x + x_0)| \le C K_0 (K+1) e^{-\delta t_0} \le K_1 e^{-\delta(t_0 + 1)}\,,$$

where $K_1 = C K_0 (K+1) e^{\delta}$. In particular, we have

$$\sup_{x \in \mathbb{R}} |\partial_x \bar{u}(x,\, t_0 + 1) - \partial_x \phi(x + x_0)| \le C K_0 (K+1) e^{-\delta t_0} \le K_1 e^{-\delta(t_0 + 1)}\,,$$

which is the same as the desired bound A.9 because $t_0 > 0$ is arbitrary. □

The following decay estimates have been proved in [14]:

Lemma A.2 ([14])**.** *Let $\bar{u}$ be the solution to A.8 and (σ^*, ϕ) be the solution to A.6. Then*

i) there exist $\mu_1, \mu_2, C > 0$ such that for $t \geq 1$, $\bar{u}$ and its derivatives satisfy

$$\begin{aligned} |\bar{u}(x,t)| + |\bar{u}_x(x,t)| + |\bar{u}_{xx}(x,t)| + |\bar{u}_t(x,t)| &\leq C(e^{-\mu_1 x} + e^{-\mu_2 t}), \quad \text{for } x > 0, \\ |1 - \bar{u}(x,t)| + |\bar{u}_x(x,t)| + |\bar{u}_{xx}(x,t)| + |\bar{u}_t(x,t)| &\leq C(e^{\mu_1 x} + e^{-\mu_2 t}), \quad \text{for } x < 0. \end{aligned} \tag{A.10}$$

ii) For the same C and μ_1 as in (i), ϕ and its derivatives satisfy

$$\begin{aligned} |\phi(x)| + |\phi_x(x)| + |\phi_{xx}(x)| &\leq Ce^{-\mu_1 x}, \quad \text{for } x > 0, \\ |1 - \phi(x)| + |\phi_x(x)| + |\phi_{xx}(x)| &\leq Ce^{\mu_1 x}, \quad \text{for } x < 0. \end{aligned} \tag{A.11}$$

It will be clear that we also need the integrability of $\bar{u}(\cdot, t)$ on $[0, \infty)$ for each t. We impose some additional decay condition on the initial data $u_0(x)$ to guarantee the integrability.

Lemma A.3. *Let $\bar{u}$ be the solution to A.8 and $u_0(x)$ be its initial datum.*

(i) When $\sigma^* > 0$, suppose there exist $\bar{x}_1$, $x_1 \geq 0$, and $q_0(x) \geq 0$ such that the initial data $u_0(x)$ in A.8 satisfies

$$\begin{aligned} u_0(x) &\leq \phi(x - \bar{x}_1) + q_0(x), \qquad \text{for all } x \geq x_1, \\ \lim_{x \to -\infty} u_0(x) &= 1, \qquad \lim_{x \to \infty} u_0(x) = 0, \end{aligned} \tag{A.12}$$

where $q_0(x) \in C^2([x_1, \infty))$ satisfies

$$\begin{aligned} 0 \leq q_0(x) \leq 1, \qquad \int_{x_1}^{\infty} q_0(x)\,\mathrm{d}x < \infty, \qquad \lim_{x \to \infty} q_0(x) = 0, \\ \sigma^* \partial_x q_0(x) + \partial_{xx} q_0(x) \leq 0, \qquad \text{for all } x \geq x_1, \end{aligned} \tag{A.13}$$

Then there exist $\bar{x}_2 \in \mathbb{R}$, $\delta_1 > 0$, and $\bar{q}_0(x) \in C^2(\mathbb{R})$ such that

$$\begin{aligned} 0 \leq \bar{q}_0(x) \leq 1, \qquad &\text{for all } x \in \mathbb{R}, \\ \bar{q}_0(x) = q_0(x), \qquad &\text{for all } x \geq x_1, \\ \sigma^* \partial_x \bar{q}_0(x) + \partial_{xx} \bar{q}_0(x) \leq 0, \quad &\text{for all } x \in \mathbb{R}, \end{aligned} \tag{A.14}$$

and the solution $\bar{u}(x,t)$ satisfies

$$0 \leq \bar{u}(x,t) \leq \phi(x - \bar{x}_2) + \bar{q}_0(x)\, e^{-\delta_1 t}. \tag{A.15}$$

(ii) When $\sigma^* = 0$, suppose there exist $\bar{x}_3 \in \mathbb{R}$, $x_3 \geq 0$, and $q_1(x) \geq 0$ such that the initial data $u_0(x)$ in A.8 satisfies

$$\begin{aligned} u_0(x) &\leq \phi(x - \bar{x}_3) + q_1(x), \qquad \text{for all } x \geq x_3, \\ \lim_{x \to -\infty} u_0(x) &= 1, \qquad \lim_{x \to \infty} u_0(x) = 0, \end{aligned} \tag{A.16}$$

where $q_1(x) \in C^2([x_3, \infty))$ satisfies

$$\begin{aligned} 0 \leq q_1(x) \leq 1, \qquad \int_{x_3}^{\infty} q_1(x)\,\mathrm{d}x < \infty, \qquad \lim_{x \to \infty} q_1(x) = 0, \\ -\tfrac{\gamma_0}{4} q_1(x) + \partial_{xx} q_1(x) \leq 0, \qquad \text{for all } x \geq x_3, \end{aligned} \tag{A.17}$$

where γ_0 is defined in A.2. Then there exist $\bar{x}_4 \in \mathbb{R}$, $\delta_2 > 0$, and $\bar{q}_1(x) \in C^2(\mathbb{R})$ such that

$$\begin{aligned} 0 \leq \bar{q}_1(x) \leq 1, \qquad &\text{for all } x \in \mathbb{R}, \\ \bar{q}_1(x) = q_1(x), \qquad &\text{for all } x \geq x_3, \\ -\tfrac{\gamma_0}{4} \bar{q}_1(x) + \partial_{xx} \bar{q}_1(x) \leq 0, \quad &\text{for all } x \in \mathbb{R}, \end{aligned} \tag{A.18}$$

and the solution $\bar{u}(x,t)$ *satisfies*

$$0 \le \bar{u}(x,t) \le \phi(x-\bar{x}_4) + \bar{q}_1(x)\, e^{-\delta_2 t}\,. \tag{A.19}$$

Remark 4. There are many possible choices for $q_0(x)$ such that A.13 can be satisfied. For example, one can choose $q_0(x) = e^{-\kappa x}$ for $0 < \kappa < \sigma^*$ and $x \ge 0$. Then A.13 is satisfied for $x_1 = 0$. One can also choose $q_0(x) = \frac{1}{1+x^2}$. Then A.13 is satisfied for x_1 large enough. Choices of $q_1(x)$ are similar.

Remark 5. One can also have lower bounds in the form $\phi(x-\bar{x}) - q(x)e^{-\delta t}$ for $\bar{u}$ in A.15 and A.19 by imposing appropriate lower bounds for the initial data. However since these explicit forms will not be used for the main result, we therefore only include the upper bound.

Now we show the proof of Lemma A.3. The idea is similar to that of Lemma 4.1 in [14]. We nevertheless include the details here for the convenience of the reader.

Proof of Lemma A.3. We show in detail the proof of the upper bound of $\bar{u}$ in A.15 for $\sigma^* > 0$. The proof for $\sigma^* = 0$ is similar. We will explain the main differences in its proof at the end.

First we construct $\bar{q}_0(x)$. Note that the reason why we need to introduce the function $\bar{q}_0(x)$ is because condition A.13 on $q_0(x)$ only imposes a bound for the tail behavior of u_0. In order to use the comparison principle as in the proof below, we need to obtain a bound for $u_0(x)$ on the whole real line.

Without loss of generality, by A.13 we can take x_1 large enough so that $q_0(x) < 1/2$ for all $x \ge x_1$. We can also assume that $q_0(x) > 0$ for all $x \ge x_1$. Otherwise, we just add an exponential function $e^{-\delta_2 x}$ to $q_0(x)$ with δ_2 small enough so that A.13 is satisfied. Furthermore, we chose x_1 such that $q_0'(x_1) \le 0$ and $q_0''(x_1) \ge 0$. This can be done because $q_0(x) \ge 0$ and $q_0(x) \to 0$ as $x \to \infty$.

The construction of $\bar{q}_0(x)$ is as follows. Let $0 < \eta_0 = 2\, q_0(x_1) < 1$. Since $\phi(x)$ is monotonously decreasing and $\lim\limits_{x\to-\infty} \phi(x) = 1$, $0 \le u_0(x) \le 1$, and $\lim_{x\to\infty} q_0(x) = 0$, there exists $x_2 \ge \bar{x}_1$ large enough such that

$$u_0(x) \le \phi(x - x_2) + \eta_0\,, \qquad \text{for all } x \in \mathbb{R}\,,$$

and

$$u_0(x) \le \phi(x - x_2)\,, \qquad \text{for } x_1 - 1 \le x \le x_1\,.$$

Here $\bar{x}_1$ is given in A.12. Define $0 \le \bar{q}_0(x) \le 1$ as

$$\bar{q}_0(x) = \begin{cases} \eta_0\,, & \text{for } x \le x_1 - 1, \\ q_0(x)\,, & \text{for } x \ge x_1\,, \\ \text{appropriate } \gamma(x), & \text{for } x_1 - 1 \le x \le x_1\,, \end{cases} \tag{A.20}$$

where $\gamma(x)$ is chosen in the way such that $\bar{q}_0(x) \in C^2(\mathbb{R})$ and A.14 is satisfied. Note that such $\gamma(x)$ always exists for $\eta_0 = 2q_0(x_1)$ and $q_0(x)$ satisfying A.13 and our previous assumptions. An explicit example is shown in Remark 6. Thus, initially we have $\bar{q}_0$ such that

$$u_0(x) \le \phi(x - x_2) + \bar{q}_0(x)\,, \qquad \text{for all } x \in \mathbb{R}\,. \tag{A.21}$$

Let $\mathcal{P}$ be the operator such that for any $w \in C^2(\mathbb{R})$,

$$\mathcal{P}w = \partial_t w - \sigma^* \partial_x w - \partial_{xx} w - f(w)\,.$$

Now we show that there exist $\delta_1 > 0$ and $z(t) \in L^\infty(\mathbb{R})$ such that

$$\mathcal{P}(\phi(x - z(t)) + \bar{q}_0(x)\, e^{-\delta_1 t}) \geq 0\,, \tag{A.22}$$

provided A.14 is satisfied. By A.6, for any $\delta_1 > 0$, $z(t) \in L^\infty(\mathbb{R})$,

$$\begin{aligned} &\mathcal{P}(\phi(x - z(t)) + \bar{q}_0(x)\, e^{-\delta_1 t}) \\ &= f(\phi(x - z(t))) - f(\phi(x - z(t)) + \bar{q}_0(x)\, e^{-\delta_1 t}) - \phi'(x - z(t))z'(t) \\ &\quad - \delta_1 e^{-\delta_1 t}\bar{q}_0(x) - e^{-\delta_1 t}(\sigma^* \partial_x \bar{q}_0(x) + \partial_{xx}\bar{q}_0(x))\,. \end{aligned} \tag{A.23}$$

In order to find some particular δ_1, $z(t)$ so that A.22 is satisfied, first notice that for each fixed t, if x is large enough then $\phi(x - z(t))$ and $\phi(x - z(t)) + \bar{q}_0(x)\, e^{-\delta_1 t}$ are both close to 0. By the definition of γ_0 in A.2, we have $f'(y) < -\gamma_0/2 < 0$ for any y which is close enough to 0. Take $0 < \delta_1 \leq \gamma_0/2$. Then

$$f(\phi(x - z(t))) - f(\phi(x - z(t)) + \bar{q}_0(x)\, e^{-\delta_1 t}) \geq \tfrac{\gamma_0}{2}\, \bar{q}_0(x)\, e^{-\delta_1 t}\,,$$

for x large enough. Together with A.14 we get

$$\mathcal{P}(\phi(x - z(t)) + \bar{q}_0(x)\, e^{-\delta_1 t}) \geq -(\delta_1 - \tfrac{\gamma_0}{2})e^{-\delta_1 t}\bar{q}_0(x) - \phi'(x - z(t))z'(t)\,.$$

If we further require that $z'(t) \geq 0$, then the monotonicity of ϕ gives

$$\mathcal{P}(\phi(x - z(t)) + \bar{q}_0(x)\, e^{-\delta_1 t}) \geq -(\delta_1 - \tfrac{\gamma_0}{2})e^{-\delta_1 t}\bar{q}_0(x) \geq 0\,.$$

The same argument holds for x negative enough because $f'(1) < 0$. Thus we can take $\delta_1 > 0$ small enough so that A.22 holds for $|x|$ large enough. Now consider the middle part where $-\infty < \bar{x} \leq x \leq \underline{x} < \infty$. Over this bounded domain for x, provided $z(t) \in L^\infty(\mathbb{R})$, there exist $\beta_1, \beta_2 > 0$ such that

$$-\infty < -\beta_1 < \phi'(x - z(t)) < -\beta_2 < 0\,.$$

Furthermore, by A.2 we have for $z'(t) \geq 0$,

$$\begin{aligned} \mathcal{P}(\phi(x - z(t)) + \bar{q}_0(x)\, e^{-\delta_1 t}) &\geq -(\delta_1 + K)\, \bar{q}_0(x)\, e^{-\delta_1 t} - \phi'(x - z(t))z'(t) \\ &\geq -(\delta_1 + K)\, \bar{q}_0(x)\, e^{-\delta_1 t} + \beta_2 z'(t)\,. \end{aligned}$$

Recall that by the construction in A.20 we have $0 \leq \bar{q}_0 \leq 1$. Thus,

$$\mathcal{P}(\phi(x - z(t)) + \bar{q}_0(x)\, e^{-\delta_1 t}) \geq -(\delta_1 + K)\, e^{-\delta_1 t} + \beta_2 z'(t)\,.$$

Therefore, if we choose

$$z(t) = x_2 + \frac{\delta_1 + K}{\delta_1 \beta_2} - \frac{\delta_1 + K}{\delta_1 \beta_2} e^{-\delta_1 t}\,, \tag{A.24}$$

such that

$$z(t) \in L^\infty(\mathbb{R})\,, \quad z(0) = x_2\,, \quad z'(t) = \frac{\delta_1 + K}{\beta_2}\, e^{-\delta_1 t} \geq 0\,,$$

then for all $t \in (0, +\infty)$

$$\mathcal{P}(\phi(x - z(t)) + \bar{q}_0(x)\, e^{-\delta_1 t}) \geq 0\,, \qquad \text{for all } x \in \mathbb{R}^1\,.$$

Together with A.21, $\phi(x - z(t)) + \bar{q}_0(x)\, e^{-\delta_1 t}$ is a supersolution by the comparison principle. Finally by the monotonicity of ϕ we have

$$\bar{u}(x) \leq \phi(x - z(t)) + \bar{q}_0(x)\, e^{-\delta_1 t} \leq \phi(x - x_2 - \tfrac{\delta_1 + K}{\delta_1 \beta_2}) + \bar{q}_0(x)\, e^{-\delta_1 t}\,.$$

Letting $\bar{x}_2 = x_2 + \frac{\delta_1 + K}{\delta_1 \beta_2}$, we finish the proof for the upper bound when $\sigma^* > 0$.

The same framework applies for the case where $\sigma^* = 0$. The main difference is as follows. The expression for $\mathcal{P}(\phi(x - z(t)) + \bar{q}_1(x)\, e^{-\delta_2 t})$ is

$$\begin{aligned} &\mathcal{P}(\phi(x - z(t)) + \bar{q}_1(x)\, e^{-\delta_2 t}) \\ &= f(\phi(x - z(t))) - f(\phi(x - z(t)) + \bar{q}_1(x)\, e^{-\delta_2 t}) - \phi'(x - z(t))z'(t) \\ &\quad - \delta_2 e^{-\delta_2 t}\bar{q}_1(x) - e^{-\delta_2 t}(\sigma^* \partial_x \bar{q}_1(x) + \partial_{xx}\bar{q}_1(x))\,. \end{aligned} \tag{A.25}$$

Since $\sigma^* = 0$, we no longer have $\sigma^* \partial_x \bar{q}_1(x) + \partial_{xx}\bar{q}_1(x) \le 0$ because $\bar{q}_1$ is not always concave. Therefore this term cannot simply be discarded as before. Instead, we do need sufficient bounds for it. The bound when $|x|$ is large comes from A.18 and

$$f(\phi(x - z(t))) - f(\phi(x - z(t)) + \bar{q}_1(x)\, e^{-\delta_2 t}) \ge \tfrac{\gamma_0}{2}\, \bar{q}_1(x)\, e^{-\delta_2 t}\,.$$

For x being finite, control of this extra term is given by appropriate construction of $z(t)$, where one changes the constant K in z in A.24 to $K + \frac{\gamma_0}{4}$. The rest of the proof is similar to the first part, thus omitted. □

Remark 6. Here we show an explicit example for $\gamma(x)$ in A.20. Recall that $q_0''(x_1) \ge 0$ by our assumptions. Define on $x_1 - \frac{\alpha}{2} \le x \le x_1$ that

$$p_1(x) = \frac{1}{3\alpha} q_0''(x_1)(x - x_1 + \tfrac{\alpha}{2})^3 + \Big(q_0'(x_1) - \frac{\alpha}{4} q_0''(x_1)\Big)\,(x - x_1 + \tfrac{\alpha}{2}) + b\,,$$

where b is chosen such that $p_1(x_1) = q_0(x_1)$ and $0 < \alpha < 1$ is small enough such that $p_1(x_1 - \frac{\alpha}{2}) < 2q_0(x_1) = \eta_0$. Such $p_1(x)$ is a C^2-extension of $q_0(x)$ onto the interval $[x_1 - \frac{\alpha}{2}, x_1]$. In addition, it satisfies

$$p_1''(x_1 - \tfrac{\alpha}{2}) = 0\,, \qquad p_1'(x) \le 0\,, \qquad p_1''(x) \ge 0\,, \qquad p_1'''(x) \ge 0\,,$$

for $x_1 - \frac{\alpha}{2} \le x \le x_1$. Thus,

$$\sigma^* p_1'(x) + p_1''(x) \qquad \text{is an increasing function on } [x_1 - \tfrac{\alpha}{2}, x_1].$$

This further implies that

$$\sigma^* p_1'(x) + p_1''(x) \le \sigma^* p_1'(x_1) + p_1''(x_1) \le 0\,, \qquad \text{for all } x \in [x_1 - \tfrac{\alpha}{2}, x_1].$$

To finish the construction of $\gamma(x)$ in A.20, we only need to let

$$\gamma(x) = \begin{cases} p_1(x)\,, & x_1 - \frac{\alpha}{2} \le x \le x_1\,, \\ p_2(x)\,, & x_1 - 1 \le x \le x_1 - \frac{\alpha}{2}\,, \end{cases} \tag{A.26}$$

where $p_2(x)$ is chosen to be concave and decreasing which gives a C^2-connection between η_0 and $p_1(x)$. This can be done, for example, by extending η_0 and $p_1(x)$ linearly until they intersect with each other. Then one can use a concave and decreasing curve to smooth the sharp corner where the two linear functions meet. Such $p_2(x)$ automatically satisfies that

$$\sigma^* p_2'(x) + p_2''(x) \le 0\,.$$

Hence $\gamma(x)$ defined in A.26 satisfies all desired properties.

A direct application of Lemma A.2 and Lemma A.3 gives an L^1 bound of $u(1-u)$ for $\sigma^* \ge 0$.

Lemma A.4. *Suppose $\sigma^* \ge 0$. Let u be the solution to A.3 with its initial data satisfying A.12 if $\sigma^* > 0$ or A.16 if $\sigma^* = 0$. Let $s(t)$ be given. Then*

i) there exists a constant $C > 0$ such that

$$\int_{s(t)}^{\infty} u(x,t)(1-u(x,t))\,\mathrm{d}x \le C(1+|s(t)|e^{-\mu_2 t})\,. \tag{A.27}$$

ii) Moreover, if $s(t)$ is a polynomial in t such that, for any $\gamma > 0$,

$$\lim_{t\to\infty} s(t)\,e^{-\gamma t} = 0\,, \qquad \lim_{t\to\infty} s(t) = -\infty\,. \tag{A.28}$$

Then for x_0, σ^* given in A.5 and A.6 with $\sigma^* \ge 0$,

$$\lim_{t\to\infty} \int_{s(t)}^{\infty} |u(x,t) - \phi(x-\sigma^* t - x_0)|\,\mathrm{d}x = 0\,. \tag{A.29}$$

Proof. By the definition of $\bar{u}$ in A.7 and $0 \le u(x,t) \le 1$,

$$\begin{aligned}\int_{s(t)}^{\infty} u(x,t)(1-u(x,t))\,\mathrm{d}x &= \int_{s(t)-\sigma^* t}^{\infty} \bar{u}(x,t)(1-\bar{u}(x,t))\,\mathrm{d}x \\ &\le \int_0^{\infty} \bar{u}(x,t)\,\mathrm{d}x + \int_{\min\{0,\,s(t)-\sigma^* t\}}^{0} (1-\bar{u}(x,t))\,\mathrm{d}x\,.\end{aligned}$$

By Lemma A.2,

$$\begin{aligned}\int_{\min\{0,\,s(t)-\sigma^* t\}}^{0} (1-\bar{u}(x,t))\,\mathrm{d}x &\le C_0\left(1+|s(t)-\sigma^* t|e^{-\mu_2 t}\right) \\ &\le C_1(1+|s(t)|e^{-\mu_2 t})\,.\end{aligned}$$

From Lemma A.3, because $\bar{q}_0$ is integrable on $[0,\infty)$ by its definition, the first term $\int_0^{\infty} \bar{u}(x,t)\,\mathrm{d}x$ satisfies

$$\int_0^{\infty} \bar{u}(x,t)\,\mathrm{d}x \le \int_0^{\infty} \phi(x-\bar{x}_2)\,\mathrm{d}x + \int_0^{\infty} \bar{q}_0(x)\,e^{-\delta_2 t}\,\mathrm{d}x \le C_2\,,$$

Adding up the above two inequalities then gives A.27.

The proof of A.29 is similar. For t large such that $s(t) < 0$,

$$\begin{aligned}&\int_{s(t)}^{\infty} |u(x,t) - \phi(x-\sigma^* t + x_0)|\,\mathrm{d}x = \int_{s(t)-\sigma^* t}^{\infty} |\bar{u}(x,t) - \phi(x+x_0)|\,\mathrm{d}x \\ \le &\int_{\sigma^* t}^{\infty} \max\{\phi(x+x_0),\ |\bar{q}_0(x)\,e^{-\delta_1 t} + \phi(x-\bar{x}_2) - \phi(x+x_0)|\}\,\mathrm{d}x \\ &+ \int_{s(t)-\sigma^* t}^{|s(t)|+\sigma^* t} |\bar{u}(x,t) - \phi(x+x_0)|\,\mathrm{d}x \\ \le &\int_{\sigma^* t}^{\infty} \phi(x+x_0)\,\mathrm{d}x + \int_{\sigma^* t}^{\infty} \bar{q}_0(x)\,e^{-\delta_1 t}\,\mathrm{d}x + \int_{\sigma^* t}^{\infty} |\phi(x+x_0) - \phi(x-\bar{x}_2)|\,\mathrm{d}x \\ &+ \int_{s(t)-\sigma^* t}^{|s(t)|+\sigma^* t} |\bar{u}(x,t) - \phi(x+x_0)|\,\mathrm{d}x \\ \le &\, C_3(e^{-\sigma^* \mu_1 t} + e^{-\delta_1 t} + |s(t)|e^{-\delta t} + \sigma^* t e^{-\delta t})\,,\end{aligned}$$

where μ_1 is defined in A.11, δ is defined in A.5, and δ_1 is in A.15. In the above estimates, the first inequality follows from the positivity of ϕ and $\bar{u}$. Whereas the last inequality follows from A.5, Lemma A.2, Lemma A.3, and the fact that $\sigma^* t + x_0 > 0$, $\sigma^* t - \bar{x}_2 > 0$ for t large enough. Thus A.29 holds by the assumption that $s(t)$ is a polynomial.

For $\sigma^* = 0$, the estimate is modified as follows. For t large such that $s(t) < 0$,

$$\begin{aligned}
&\int_{s(t)}^{\infty} |u(x,t) - \phi(x - \sigma^* t + x_0)| \, \mathrm{d}x = \int_{s(t)}^{\infty} |\bar{u}(x,t) - \phi(x + x_0)| \, \mathrm{d}x \\
&\leq \int_{|s(t)|}^{\infty} \max\{\phi(x + x_0),\ |\bar{q}_1(x)\, e^{-\delta_3 t} + \phi(x - \bar{x}_5) - \phi(x + x_0)|\} \, \mathrm{d}x \\
&\quad + \int_{s(t)}^{|s(t)|} |\bar{u}(x,t) - \phi(x + x_0)| \, \mathrm{d}x \\
&\leq C_3 (e^{-\mu_1 |s(t)|} + e^{-\delta_3 t} + |s(t)| e^{-\delta t}) \,,
\end{aligned} \tag{A.30}$$

which then completes the proof. □

Now we proceed to prove Proposition 1, 2, 3.

Proof of Proposition 1. Let $u(x,t)$ be the solution to A.3 with the initial $u_0(x) = v_0(x)$. Notice that if there exists a unique $\sigma(t)$ in 2.6 for all t, then by the uniqueness of the solution to A.3, $(\sigma,\, u(x + \int_0^t \sigma(s)\, \mathrm{d}s))$ is the unique solution to 2.6. Thus the existence and uniqueness of (σ, v) reduces to the existence and uniqueness of σ. Expressed in terms of u, the equation for σ is

$$\sigma(t) = \tfrac{1}{\epsilon} \left(-\partial_x u \left(\int_0^t \sigma(s)\, \mathrm{d}s,\, t \right) + \int_{\int_0^t \sigma(s)\, \mathrm{d}s}^{\infty} f(u)\, \mathrm{d}x \right) . \tag{A.31}$$

Recall that $u(x,t)$ is the solution to A.3 which is a known function by Theorem A.1 from [14]. Thus, if we let $r(t) = \int_0^t \sigma(s)\, \mathrm{d}s$, then $r(t)$ satisfies an ordinary differential equation

$$r'(t) = \tfrac{1}{\epsilon} \left(-\partial_x u\, (r(t),\, t) + \int_{r(t)}^{\infty} f(u)\, \mathrm{d}x \right) \equiv F(r,t) \,, \qquad r(0) = 0 \,. \tag{A.32}$$

If we are able to show that $|\sigma(t)|$ is uniformly bounded by a constant, then the uniform bound of u and the interior Schauder estimates (or Lemma A.2) indicate $F(r,t)$ is uniformly Lipschitz in r. Therefore there exists a unique $r(t)$ for all $t \geq 0$. Then from $\sigma(t) = r'(t)$ there exists a unique $\sigma(t)$ for all time. This gives the existence and uniqueness of the solution (σ, v).

The rest of the proof is to show a priori bounds for $r(t)$ and $\sigma(t)$. By A.1, Lemma A.4, and the fact that $\partial_x u \leq 0$, we have

$$r'(t) \geq \tfrac{1}{\epsilon} \int_{r(t)}^{\infty} f(u)\, \mathrm{d}x \geq -\tfrac{C_\alpha}{\epsilon} \int_{r(t)}^{\infty} u(1-u)\, \mathrm{d}x \geq -C_4 (1 + |r(t)| e^{-\mu_2 t}) \,. \tag{A.33}$$

Choose t_0 large enough such that

$$t e^{-\mu_2 t} \leq \frac{1}{2C_4} \,, \qquad \text{for all } t \geq t_0 \,.$$

Fix t_0 and suppose that for some $C_5 > 2C_4 > 0$, we have $r(t) \geq -(C_5 - 1)t$ for $t \in [0, t_0]$. Note that such C_5 exists because $r(0) = 0$. We want to show that $r(t) \geq -C_5 t$ for all $t \geq 0$. To this end, suppose $t_1 \geq t_0$ satisfies that $r(t_1) = -C_5 t_1$. Then

$$r'(t_1) \geq -C_4 (1 + C_5 t_1 e^{-\mu_2 t_1}) \geq -C_4 \left(1 + \frac{1}{2C_4} C_5 \right) = -C_4 - \frac{C_5}{2} \geq -C_5 \,.$$

Hence we have

$$r(t) \geq -C_5 t \,, \qquad \text{for all } t \geq 0 \,. \tag{A.34}$$

Hence by A.1 and Lemma A.4, the integral term $\int_{r(t)}^{\infty} f(u)\,\mathrm{d}x$ is well-defined and uniformly bounded for all t. The first term $-\partial_x u\left(\int_0^t \sigma(s)\,\mathrm{d}s,\, t\right)$ in A.31 is also uniformly bounded for all t by the interior Schauder estimates (or Lemma A.2). We thus have that there exists a constant $C > 0$ such that

$$|\sigma(t)| \le C\,, \qquad \text{for all } t \ge 0\,.$$

By the argument before the a priori bounds, we thereby finish the proof. □

Next we show the convergence of (σ, v).

Proof of Proposition 2. u, ϕ are the solutions to A.3 and A.6 respectively. Let

$$A(t) = \int_0^t \sigma(s)\,\mathrm{d}s - \sigma^* t + x_0\,, \tag{A.35}$$

where x_0 is given in A.5. First we show that $A(t)$ is uniformly bounded in t. By A.32 the equation of $A(t)$ is

$$A'(t) = \tfrac{1}{\epsilon}\left(-\partial_x u\left(A(t) + \sigma^* t - x_0,\, t\right) + \int_{A(t)+\sigma^* t - x_0}^{\infty} f(u)\,\mathrm{d}x\right) - \sigma^*\,, \quad A(0) = x_0\,.$$

Using $\bar{u}(x,t) = u(x + \sigma^* t, t)$, we have

$$A'(t) = \tfrac{1}{\epsilon}\left(-\partial_x \bar{u}\left(A(t) - x_0,\, t\right) + \int_{A(t)-x_0}^{\infty} f(\bar{u})\,\mathrm{d}x\right) - \sigma^*\,, \qquad A(0) = x_0\,.$$

If we write the above equation in terms of the traveling front ϕ, then

$$A'(t) = \tfrac{1}{\epsilon}\left(-\partial_x \phi\left(A(t),\, t\right) + \int_{A(t)}^{\infty} f(\phi)\,\mathrm{d}x\right) - \sigma^* + \tilde{R}(t)\,, \tag{A.36}$$

with $\tilde{R} = \tilde{R}_1 + \tilde{R}_2$ such that

$$\begin{aligned}
\tilde{R}_1 =& -\tfrac{1}{\epsilon}\left(\partial_x \bar{u}(A(t) - x_0, t) - \partial_x \phi(A(t), t)\right)\,,\\
\tilde{R}_2 =& \tfrac{1}{\epsilon}\left(\int_{A(t)-x_0}^{\infty} f(\bar{u})\,\mathrm{d}x - \int_{A(t)}^{\infty} f(\phi)\,\mathrm{d}x\right)\\
=& \tfrac{1}{\epsilon}\int_{\int_0^t \sigma(s)\,\mathrm{d}s}^{\infty} \left(f(u) - f(\phi(x - \sigma^* t + x_0))\right)\mathrm{d}x\,.
\end{aligned} \tag{A.37}$$

By Corollary 1,

$$\tilde{R}_1(t) \to 0\,, \qquad \text{as } t \to \infty\,. \tag{A.38}$$

Meanwhile by A.2, A.34, and Lemma A.4,

$$\begin{aligned}
|\tilde{R}_2(t)| &\le \tfrac{K}{\epsilon}\int_{\int_0^t \sigma(s)\,\mathrm{d}s}^{\infty} |u(x,t) - \phi(x - \sigma^* t + x_0)|\,\mathrm{d}x\\
&\le \tfrac{K}{\epsilon}\int_{-C_6 t}^{\infty} |u(x,t) - \phi(x - \sigma^* t + x_0)|\,\mathrm{d}x \to 0\,, \qquad \text{as } t \to \infty\,.
\end{aligned} \tag{A.39}$$

Combining A.38 and A.39 we have

$$\tilde{R}(t) \to 0\,, \qquad \text{as } t \to \infty\,. \tag{A.40}$$

Notice that if we integrate equation A.6 for ϕ from $A(t)$ to ∞, then

$$-\partial_x \phi\left(A(t),\, t\right) + \int_{A(t)}^{\infty} f(\phi)\,\mathrm{d}x = \sigma^* \phi(A(t))\,.$$

Therefore equation A.36 becomes

$$A'(t) = \tfrac{\sigma^*}{\epsilon}\phi(A(t)) - \sigma^* + \tilde{R}(t)\,, \qquad A(0) = x_0\,. \tag{A.41}$$

If there exists $\delta_0 > 0$ such that

$$\phi'(A(t)) < -\delta_0\,, \qquad \text{for all } t \geq 0, \tag{A.42}$$

we can show that $A(t) \to 0$ as $t \to \infty$. By A.41,

$$\frac{\mathrm{d}}{\mathrm{d}t}(\phi(A(t)) - \epsilon) = \tfrac{\sigma^*}{\epsilon}\phi'(A(t))(\phi(A(t)) - \epsilon) + \phi'(A(t))\tilde{R}(t)\,.$$

Multiplying the above equation by $\operatorname{sgn}(\phi(A(t)) - \epsilon)$ and using A.42, we have

$$\begin{aligned}\frac{\mathrm{d}}{\mathrm{d}t}|\phi(A(t)) - \epsilon| &= \tfrac{\sigma^*}{\epsilon}\phi'(A(t))\,|\phi(A(t)) - \epsilon| + \operatorname{sgn}(\phi(A(t)) - \epsilon)\phi'(A(t))\tilde{R}(t) \\ &\leq -\tfrac{\sigma^*\delta_0}{\epsilon}|\phi(A(t)) - \epsilon| + C|\tilde{R}(t)|\,.\end{aligned}$$

This gives

$$|\phi(A(t)) - \epsilon| \leq e^{-\frac{\sigma^*\delta_0}{\epsilon}t}|\phi(x_0) - \epsilon| + C\int_0^t e^{-\frac{\sigma^*\delta_0}{\epsilon}(t-s)}|\tilde{R}(s)|\,\mathrm{d}s\,. \tag{A.43}$$

By A.40, the second term involving $\tilde{R}(s)$ in A.43 approaches zero as $t \to \infty$. This can be seen by considering the integral on $[0,\, t/2]$ and $[t/2,\, t]$ respectively. Therefore,

$$|\phi(A(t)) - \epsilon| \to 0\,, \qquad \text{as } t \to \infty\,. \tag{A.44}$$

Due to the monotonicity of ϕ and $\phi(0) = \epsilon$, A.44 is equivalent to

$$A(t) \to 0\,, \qquad \text{as } t \to \infty\,.$$

By A.41 this implies $A'(t) \to 0$, that is, $\sigma(t) \to \sigma^*$ as $t \to \infty$. Furthermore, by the uniform convergence in A.5,

$$v(x,t) = u(x + A(t) + \sigma^* t - x_0, t) \to \phi(x)\,, \qquad \text{as } t \to \infty\,.$$

The only rest part is to show the existence of δ_0 in A.42. This is achieved by proving that $A(t)$ is uniformly bounded for all $t \geq 0$. In order to show that $A(t)$ is bounded from above, fix $t_3 > 0$ such that $|\tilde{R}| < \frac{\sigma^*}{4}$ for all $t \geq t_3$. If there exist $t_4 \geq t_3$ and $x_1 > 0$ such that $\phi(x_1) < \frac{\epsilon}{2}$ and $A(t_4) = x_1$, then

$$A'(t_2) = \tfrac{\sigma^*}{\epsilon}\phi(A(t_2)) - \sigma^* + \tilde{R}(t_2) \leq \tfrac{\sigma^*}{2} - \sigma^* + \frac{\sigma^*}{4} < 0\,.$$

This means $A(t)$ will decrease at t_4. Thus $A(t) \leq x_1$ for all $t > t_4$. Similar argument shows $A(t)$ also has a lower bound for all $t \geq 0$. Since $\phi'(x) < 0$ for any $x \in \mathbb{R}$, there exists δ_0 such that A.42 holds. We thereby finish the convergence proof. □

Finally we show the proof of Proposition 3.

Proof of Proposition 3. When $\sigma^* = 0$, let u be the solution to A.3 with $u_0(x) = v_0(x)$ and x_0 the number in A.5. For $\sigma^* = 0$, the quantity $A(t)$ is defined as

$$A(t) = \int_0^t \sigma(s)\,\mathrm{d}s + x_0\,, \tag{A.45}$$

It satisfies a similar equation as A.36:

$$A'(t) = \tfrac{1}{\epsilon}\left(-\partial_x\phi\,(A(t),\, t) + \int_{A(t)}^{\infty} f(\phi)\,\mathrm{d}x\right) + \tilde{R}(t)\,, \qquad A(0) = x_0\,, \tag{A.46}$$

where $\tilde{R} = \tilde{R}_1 + \tilde{R}_2$ such that

$$\begin{aligned} \tilde{R}_1 &= -\tfrac{1}{\epsilon}\left(\partial_x u(A(t)-x_0,t) - \partial_x \phi(A(t),t)\right), \\ \tilde{R}_2 &= \tfrac{1}{\epsilon}\int_{\int_0^t \sigma(s)\,\mathrm{d}s}^{\infty} \left(f(u(x)) - f(\phi(x+x_0))\right)\mathrm{d}x\,. \end{aligned} \tag{A.47}$$

Notice that in this case $u = \bar{u}$. Since the bounds A.9, A.34, and Lemma A.4 still hold for $\sigma^* = 0$, we have as before

$$\tilde{R}(t) \to 0\,, \qquad \text{as } t \to \infty\,.$$

By integrating equation A.6 for ϕ with $\sigma^* = 0$, the first term on the right hand side of A.46 vanishes. Due to the loss of this stabilizing term, the limiting profile (if exists) is not unique. This is in contrast to the case when $\sigma^* > 0$. Nevertheless we can still show that $\sigma(t) \to 0$ as $t \to \infty$. This is simply because that by the definition of $A(t)$ in A.45 we have

$$\sigma(t) = A'(t) = \tilde{R}(t) \to 0\,, \qquad \text{as } t \to \infty.$$

We can also show that the solution v to 2.6 converges to a certain shift of ϕ. Unlike the case when $\sigma^* > 0$, now the amount of shift depends on particular initial data of v. This convergence follows from a slightly more detailed estimate of R_1, R_2. By A.9,

$$|R_1(t)| \le \tfrac{K_1}{\epsilon}\, e^{-\delta t}\,. \tag{A.48}$$

A similar calculation as in A.39 gives

$$|R_2(t)| \le \tfrac{K}{\epsilon}\int_{-C_6 t}^{\infty} |u(x,t)-\phi(x+x_0)|\,\mathrm{d}x \le \tfrac{KC_3}{\epsilon}(e^{-\mu_1 C_6 t}+e^{-\delta_3 t}+C_6 t e^{-\delta t})\,, \tag{A.49}$$

where the last inequality follows from A.30. These two bounds show that $R_1, R_2 \in L^1(0,\infty)$. Therefore $A(t) = x_0 + \int_0^t (R_1+R_2)(s)\,\mathrm{d}s$ is uniformly bounded for $t \in [0,\infty)$ and is a Cauchy sequence in t. Consequently, there exists $a_0 \in \mathbb{R}$ such that

$$A(t) \to a_0 \qquad \text{as } t \to \infty.$$

Recall that u is the solution to A.3 with initial data $u_0(x) = v_0(x)$ which converges to $\phi(x+x_0)$. By the uniform continuity of u, the sequence $v(x,t) = u(x+A(t),t)$ converges uniformly in x to $\phi(x+a_0)$ as $t \to \infty$, which proves the claim that $v(x,t)$ converges to a shift a_0 of ϕ as $t \to \infty$ with a_0 depending on v_0. □

Remark 7. One can see from the proofs of Proposition 2 and 3 that the essence for both proofs is that the remainder terms $R_1, R_2 \to 0$ as $t \to \infty$. By the definitions for R_1, R_2, this is equivalent to require that the original solution $\bar{u}$ converges fast enough to the traveling front ϕ (up to a shift). Since there are very few cases where the convergence rate is explicitly known, this only provides a formal argument of the convergence of our scheme.

Appendix B. **Necessity of the proper choice of $\mathfrak{P}$.** In this part we justify the choice of integration interval $[0,\infty)$ instead of $(-\infty,0]$ when σ^* is positive for the whole space case. This can be seen by studying a similar equation as A.36 for $A(t)$. Recall the definition of $A(t)$ in A.35:

$$A(t) = \int_0^t \sigma(s)\,\mathrm{d}s - \sigma^* t + x_0\,.$$

If we choose the integration interval as $(-\infty, 0]$ in 2.6, then $\sigma(t)$ is defined as

$$\sigma = \tfrac{1}{1-\epsilon}\left(\partial_x v(0,t) + \int_{-\infty}^{0} f(v)\,\mathrm{d}x\right).$$

We prove by contradiction that the system 2.6 with the so-defined σ will not converge to a positive σ^*. Assume that the scheme still converges: $\sigma(t)$ is bounded for all $t \geq 0$ and

$$\lim_{t\to\infty} v(x,t) = \phi\,, \qquad \lim_{t\to\infty} \sigma(t) = \sigma^* > 0\,.$$

The equation for $A(t)$ now has the form

$$A'(t) = \tfrac{1}{1-\epsilon}\left(\partial_x \phi\left(A(t),\, t\right) + \int_{-\infty}^{A(t)} f(\phi)\,\mathrm{d}x\right) - \sigma^* + \hat{R}(t)\,, \tag{B.1}$$

where $\hat{R} = \hat{R}_1 + \hat{R}_2$ such that

$$\begin{aligned}
\hat{R}_1 =& \tfrac{1}{1-\epsilon}\left(\partial_x \bar{u}(A(t) - x_0, t) - \partial_x \phi(A(t), t)\right)\,,\\
\hat{R}_2 =& \tfrac{1}{\epsilon}\left(\int_{-\infty}^{A(t)-x_0} f(\bar{u})\,\mathrm{d}x - \int_{-\infty}^{A(t)} f(\phi)\,\mathrm{d}x\right)\\
=& \tfrac{1}{\epsilon}\int_{-\infty}^{\int_0^t \sigma(s)\,\mathrm{d}s} \left(f(u(x)) - f(\phi(x - \sigma^* t + x_0))\right)\mathrm{d}x\,.
\end{aligned} \tag{B.2}$$

By Remark 5 one can show that for appropriate initial data for u, the remainder term $\hat{R}$ is well-defined and satisfies $\hat{R} \to 0$ as $t \to \infty$. Thus similar as in A.36, the main properties of $A(t)$ are dictated by the first two terms in B.1. Integrating the equation for ϕ from $-\infty$ to $A(t)$, we get

$$A'(t) = -\tfrac{\sigma^*}{1-\epsilon}\left(\phi(A(t) + (1-\epsilon))\right) + \hat{R}\,.$$

Since $\phi(\cdot) \geq 0$ and $\hat{R} \to 0$ as $t \to \infty$, for any $\gamma > 0$, there exists $t_\gamma > 0$ such that

$$\sigma(t) - \sigma^* = A'(t) \leq -\sigma^* + \gamma\,, \qquad \text{for any } t \geq t_\gamma.$$

Thus

$$\sigma(t) < \gamma\,, \qquad \text{for any } t \geq t_\gamma.$$

Since $\gamma > 0$ is arbitrary, we have

$$\limsup_{t\to\infty} \sigma(t) \leq 0\,,$$

which contradicts the assumption that $\lim_{t\to\infty} \sigma(t) = \sigma^* > 0$. Therefore for $\sigma^* > 0$, it is necessary to choose the integration interval as $[0, \infty)$ instead of $(-\infty, 0]$. For the bounded domain this then suggests to choose $[0, x_r]$ when $\sigma^* > 0$ and $[x_l, 0]$ when $\sigma^* < 0$. Both choices work if $\sigma^* = 0$.

Acknowledgments. The second author would like to thank Professor Benoit Perthame at UPMC for useful discussions when initiating this work. Both authors want to thank IPAM for organizing the long term programm "Quantum and Kinetic Transport". This collaborated work started when both authors attended the first reunion for this programme.

REFERENCES

[1] H. Berestycki, *The influence of advection on the propagation of fronts in reaction-diffusion equations*, Nonlinear PDEs in Condensed Matter and Reactive Flows, NATO Science Series C, **569**, (eds. H. Berestycki and Y. Pomeau), Kluwer, Dordrecht, (2003).

[2] H. Berestycki and F. Hamel, *Front propagation in periodic excitable media*, Comm. Pure Appl. Math., **55** (2002), 949–1032 .

[3] H. Berestycki, B. Larrouturou and J.-M. Roquejoffre, *Mathematical investigation of the cold boundary difficulty in flame propagation theory*, Dynamical Issues in Combustion Theory (Minneapolis, MN, 1989), 37–61, IMA Vol. Math. Appl., **35**, Springer, New York, (1991).

[4] H. Berestycki, G. Nadin, B. Perthame and L. Ryzhik, *The non-local Fisher-KPP equation: traveling waves and steady states*, Nonlinearity, **22** (2009), 2813–2844.

[5] H. Berestyski, B. Nicolaenko and B. Scheurer, *Traveling wave solutions to combustion models and their singular limits*, SIAM J. Math. Anal, **16** (1985), 1207–1242.

[6] J. Billingham and N. L. Needham, *The development of traveling waves in quadratic and cubic autocatalysis with unequal diffusion rates. I. Permamnet form traveling waves*, Phil. Trans. R. Soc. Lond. A, **334** (1991), 1–24.

[7] V. Gubernov, G. N. Mercer, H. S. Sidhu and R. O. Weber, *Numerical methods for the traveling wave solutions in reaction diffusion equations*, ANZIAM J., **44** (2002), 271–299.

[8] F. Bouchut, "Nonlinear Stability of Finite Volume methods for Hyperbolic Conservation Laws and Well-Balanced Schemes for Sources," Series Frontiers in Mathematics, Birkhäuser Verlag, Basel, 2004.

[9] F. Cerreti, B. Perthame, C. Schmeiser, M. Tang and N. Vauchelet, *Waves for an hyperbolic Keller-Segel model and branching instabilities*, Math. Models and Meth. in Appl. Sci., **21** (2011), 825–842.

[10] J. Demmel, L. Dieci and M. Friedman, *Computing connecting orbits via an improved algorithm for continuing invariant subspaces*, SIAM J. Sci. Comp., **22** (2000), 81–94.

[11] E. J. Doedel, M. J. Friedman and B. I. Kunin, *Successive continuation for locating connecting orbits*, Numer. Algorithms, **14** (1997), 103–124.

[12] M. A. Fuentes, M. N. Kuperman and V. M. Kenkre, *Nonlocal interaction effects on pattern formation in population dynamics*, Phys. Rev. Lett., **91** (2003), 158104.

[13] R. A. Fisher, "The Genetical Theory of Natural Selection," Clarendon Press, 1930. second edition: Dover, 1985. Third edition, Oxford Univ. Press, 1999.

[14] P. C. Fife and J. B. Mcleod, *The approach of solutions of non-linear diffusion equations to traveling front solutions*, Arch. Ration. Mech. Anal., **65** (1977), 335–361.

[15] A. N. Kolmogorov, I. G. Petrovskii and N. S. Piskunov, *Etude de l équation de la diffusion avec croissance de la quantité de matière et son application à un problème biologique*, Bulletin Université d'Etat à Moscou (Bjul. Moskouskogo Gos. Univ.), (1937), 1–26.

[16] S. Genieys, V. Volpert and P. Auger, *Pattern and waves for a model in population dynamics with nonlocal consumption of resources*, Math. Modelling Nat. Phenom., **1** (2006), 65–82.

[17] G. M. Lieberman, "Second Order Parabolic Differential Operators," World Scientific Publishing. Co. Singapore, 1996.

[18] W. Malfliet, *Travelling-wave solutions of coupled nonlinear evolution equations*, Mathematics and Computers in Simulation, **62** (2003), 101–108.

[19] G. Nadin, B. Perthame and M. Tang, *Can a traveling wave connect two unstable states? The case of the nonlocal Fisher equation*, C. R. Acad. Sci. Paris I, **349** (2011), 559–557.

[20] G. Nadin, *Pulsating traveling fronts in space-time periodic media*, C. R. Acad. Sci. Paris I, **346** (2008), 951–956.

[21] J. Nolen and J. Xin, *Reaction-diffusion front speeds in spatially-temporally periodic shear flows*, SIAM J. Multiscale Modeling and Simulation, **1** (2003), 554–570.

[22] B. Perthame, C. Schmeiser, M. Tang and N. Vauchelet, *Traveling plateaus for a Keller-Segel system with logistic sensitivity; Existence and branching instabilities*, Nonlinearity, **24** (2011), 1253–1270.

[23] B. Perthame, "Transport Equations in Biology," (LN Series Frontiers in Mathematics), Birkhauser, 2007.

[24] M. Sermange, *Mathematical and numerical aspects of one-dimensional laminar flame simulation*, Appl. Math. Optim., **14** (1986), 131–153.

[25] G. Samaey, K. Engelborghs and D. Roose, *Numerical computation of connecting orbits in delayed differential equations*, Numerical Algorithms, **30** (2002), 335–352.

[26] M. D. Smooke, J. A. Miller and R. J. Kee, *Determination of adiabatic flame speeds by boundary value methods*, Combustion Sci. and Technology, **34** (1983), 79–90.
[27] M. Tang, *A relaxation method for the pulsating traveling front simulations of the space and time periodic advection diffusion reaction equations*, Communications in Mathematical Sciences, Accepted.

Received June 2012; revised November 2012.

E-mail address: weirans@sfu.ca
E-mail address: tangmin@sjtu.edu.cn